CHALMERS
UNIVERSITY OF TECHNOLOGY

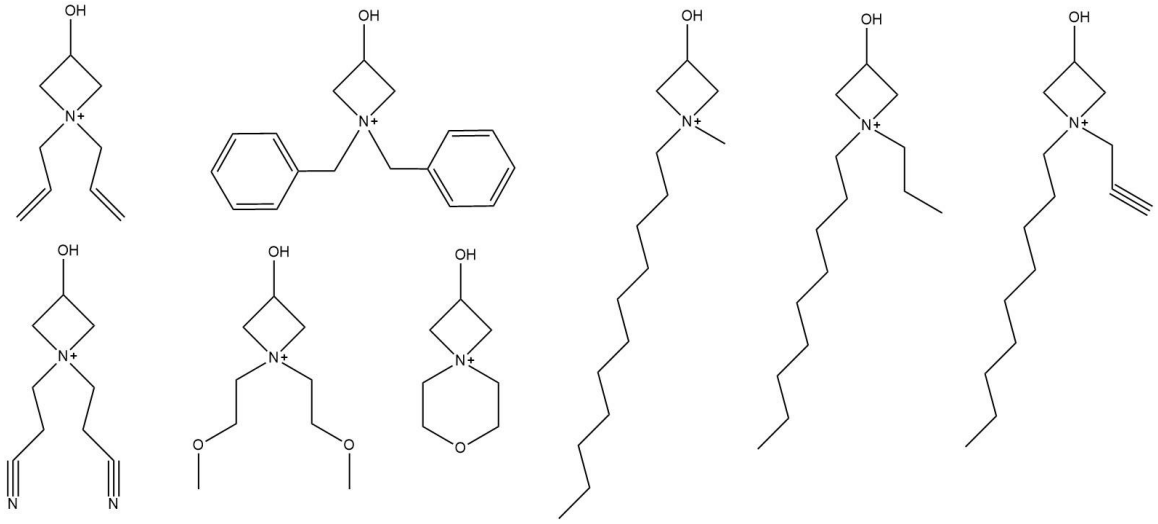

Design and synthesis of azetidinium salts for chemical modification of nanocrystalline cellulose

Master's thesis in Materials Chemistry

PATRIK ROSENDAHL

Department of Chemistry and Chemical Engineering
Division of Chemistry and Biochemistry, Organic Chemistry
CHALMERS UNIVERSITY OF TECHNOLOGY
Gothenburg, Sweden 2017

Design and synthesis of azetidinium salts for chemical modification of nanocrystalline cellulose
PATRIK ROSENDAHL

Supervisors: Filip Nylander, Karin Sahlin, Department of Chemistry and Chemical Engineering.
Examiner: Gunnar Westman, Department of Chemistry and Chemical Engineering.

Master's Thesis 2017
Department of Chemistry and Chemical Engineering
Division of Chemistry and Biochemistry
Chalmers University of Technology
SE-412 96 Gothenburg
Sweden
Telephone + 46 (0)31-772 1000

Cover: Synthesized azetidinium salts. Top row from the left: diallylazetidinium salt, dibenzylazetidinium salt, undecylmethylazetidinium salt, nonylpropylazetidinium salt, nonylpropatgylazetidinium salt. Bottom row from the left: 3,3'-Iminodipropionitrileazetidinium salt, bis(2-methoxyehyl)azetidinium salt and morpholineazetidinium salt.

Gothenburg, Sweden 2017

Abstract

Increasing demands for new recyclable biomaterials have made it more important to find alternatives to fossil based materials. Nanofibrillated cellulose (CNF) and nanocrystalline cellulose (CNC) are cellulosic materials with at least one dimension in the nanoscale. They can be functionalized with carboxyl or sulfate groups which produces a charged nanocellulose material that could potentially be used in the production of biobased materials in the future. Azetidinium salts are a possible candidate for modification of sulfated nanocrystalline cellulose and could be used in biocomposite materials with improved thermal and mechanical properties.

Azetidinium salts consists of four-atom ring that can react under mild conditions with sulfate groups on nanocrystalline cellulose via nucleophilic attack. The end groups on azetidinium salts can be designed to fit the desired application and give the material new improved properties.

In this project was the synthesis of different symmetrical and asymmetrical azetidinium salts investigated under different reaction conditions. Parameters that were evaluated was temperature and solvents with the aim to find optimal reaction conditions. Different asymmetrical secondary amines were prepared by reductive amination of aldehydes and used to synthesize asymmetrical salts with different side groups.

The synthesized azetidinium salts were evaluated with ^{1}H-NMR and successful products were achieved for several of the salts tested. Results showed that there weren't any single optimal reaction settings that worked for all azetidinium salts. Instead it varied for each azetidinium salt. Modification of nanocrystalline cellulose with diallylazetidinium salt was verified with FTIR and Zeta potential measurement. Thiol-functionalisation of diallyl-CNC was also performed and successful modification was indicated by FTIR.

The study shows that the azetidinium salts could potentially be used in biocomposite applications in the future. By developing and understanding reaction mechanism behind the azetidinium salts they could become an important part of tomorrow's materials.

Acknowledgements

The work behind this thesis has been carried out at Organic Chemistry in the division for Chemistry and Biochemistry at Chalmers University of Technology during the spring of 2017. I want to give a special thanks to Gunnar Westman who has been my examiner and guided the project. Your support and feedback has been much appreciated. I also want to thank Filip Nylander and Karin Sahlin who have been my supervisors and helped me with the laboratory work and answered a lot of questions. Lastly, I want to thank Robin Nilsson who have helped with the modification of CNC as well as the other thesis students at Organic Chemistry for inspiration, discussions and a good time during this spring.

Patrik Rosendahl, Gothenburg, May 2017

Table of contents

1. Introduction

The strive for newer and better materials that's also recyclable have led to increasing amount of research into development of new biobased materials. They are of interest due to their potential use in biocomposites. Biocomposites are a class of composites that consists of a matrix and natural fibers. The extensive use of petroleum products has led to problems with depletion of oil but also environmental concerns of microplastics polluting the environment. Replacing petroleum products with purely biobased materials are not a viable option due to economic aspects. A more suitable solution would be to combine petroleum and biobased materials to produce more cost effective biodegradable biocomposites consisting of natural fibers mixed with synthetic polymers. These biocomposites could be a solution to several of these problems and concerns regarding the extensive use of synthetic petroleum based polymers. In order to achieve this, the biopolymers need to be modified to become compatible with the synthetic polymers used in the matrix of biocomposite materials. [1]

Materials such as polysaccharides have been of interest due to them occurring naturally in abundance[2]. Different variants of polysaccharides exist in nature such as functionalized polysaccharides which have been investigated for several decades[3]. Examples of functionalized polysaccharides are sulfated nanocrystalline cellulose (CNC) which can be produced by mixing cellulose and sulfuric acid which leads to hydrolysis of the cellulose into nanocrystals with substituted hydroxyl groups. The hydroxyl groups get replaced with charged sulfate groups which changes the properties of the cellulose. Sulfated nanocellulose is highly hydrophilic and in order to be able to mix it in hydrophobic matrices used in biocomposites they need to be modified. If not, the CNC can form aggregates which prevents dispersion in the matrix[4]. This can be prevented in two ways, by adsorption of a hydrophobic cation to the anionic sulfate groups or by chemical modification of the nanocrystalline cellulose. Chemical modification is performed by functionalization of the hydroxyl groups on the cellulose. However, this leaves the anionic sulfate group on the cellulose which can inhibit the mixing with the matrix and thereby cause poorer performance of the biocomposite. [5]

By focusing on adsorption and conjugation of the sulfate group, this problem can be solved. In this project, the interaction between the sulfated CNC and azetidinium salts was investigated. Azetidinium salts consists of a 4-atom ring where the positive charge of the azetidinium salts interacts with the negative sulfate group and thus enables adsorption. The sulfated CNC ester works as a nucleophile ring-opener of the azetidinium salt while the ring-structure of four atoms of the salt enables reaction during mild conditions. [5]

This thesis investigated the synthesis of azetidinium salts under different reaction conditions and synthesis of a variety of these salts with different side groups. By designing different side groups on the azetidinium salt it's possible to fine tune the interaction of modified-CNC and the matrix in biocomposites. This can be done by choosing side groups that improves mixability with the matrix and enable degradability of the composite while keeping the mechanical properties intact. [5]

1.1. Aims

This project aimed to explore a new type of reactions between azetidinium salts and their connection to sulfated nanocrystalline cellulose. The project included investigating how chemical groups in azetidinium salts affect the CNC compatibility with biocomposite matrices and to seek reaction conditions that make it possible to make these reactions on a bigger scale. The project aimed to verify what type of azetidinium salts that can be synthesized under mild conditions and to synthesize a variety of salts with different side groups to increase understanding of the reaction mechanisms behind them.

1.2. Limitations

The project was limited to only use sulfated CNC as ring-opener of azetidinium salts.
The azetidinium salts were limited to some symmetrical and asymmetrical depending on what starting material was available. Not much research has been done in this area which limited the project to simple structures. The large-scale experiments for synthesis of azetidinium salts were limited to about 0.1 kg due to limits in available chemicals.

2. Theory

This section covers theoretical background behind this thesis. Theory about cellulose and sulfated nanocrystalline cellulose as well as azetidinium salts is presented in this chapter. Lastly theory covering modification of CNC is presented.

2.1 Cellulose

Cellulose is one of the most abundant polysaccharides on earth and is used to produce many different materials such as plastics and paper products. Cellulose has the molecular formula $(C_6H_{10}O_5)_n$ and is a linear polysaccharide consisting of long crystalline chains of several thousand D-glucose subunits linked together with β(1→4) bonds. The glucose chains in cellulose are arranged in a way that forms orderly crystals which aggregate and form cellulose fibrils. These fibrils are impermeable to water and this makes the cellulose insoluble and resistant to hydrolysis[6]. Each anhydroglucose unit consists of three reactive hydroxyl side groups. These hydroxyl groups can be substituted and a measure of this is degrees of substitution (DS) which for cellulose can have values between 0 and 3. [7] The molecular structure of cellulose can be seen in figure 1.

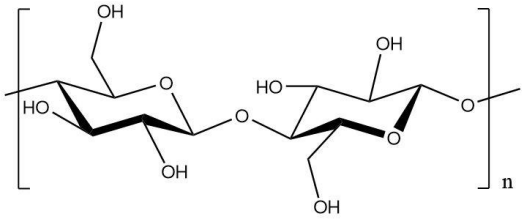

Figure 1 - Chemical structure of cellulose[8]

2.1.1 Nanocrystalline cellulose, CNC

CNC is prepared from microfibrillated cellulose that is treated with sulfuric acid. The treatment hydrolyses the microfibrillated cellulose into charged nanocrystals where some of the hydroxyl groups gets replaced with sulfuric ester groups ($-OSO_3^-$) which causes formation of stable aqueous CNC suspensions[5]. The cellulose fibers are semi-crystalline which means that they consist of crystalline and amorphous regions. The amorphous regions are areas of disorientation with lower density and act as structural defects which are sensitive to acid attack. The amorphous areas are permeable to the hydronium ions which promote hydrolytic breakdown of the β(1→4) bonds. The hydrolysis leads to cleavage in the amorphous regions and this leads to formation of single crystallites. The sulfuric acid also reacts with the free hydroxyl groups in an esterification process where charged sulfate ester groups get distributed randomly on the nanocrystal surface. The presence of these charged ester groups induce electrostatic repulsion between the

nanocrystals and this increases their ability to be dispersed in water[8]. The esterification reaction can be seen in figure 2 below.

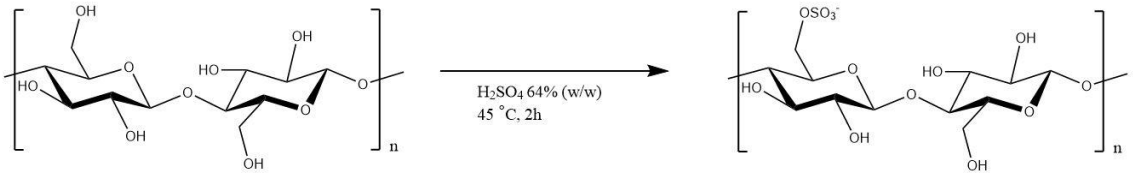

Figure 2 - Hydrolysis of cellulose into sulfated nanocrystalline cellulose by treatment with sulfuric acid. Some of the hydroxyl groups get replaced with charged sulfuric groups in an esterification reaction.[5]

Although the hydrolysis produces short crystalline cellulose nanoparticles they still contain amorphous regions. The degree of crystallinity in the CNC can be measured with powder X-ray diffraction. The percentage of crystallinity (%Cr) can be calculated with equation 1 where I_{am} is the diffraction intensity for the amorphous material taken at the 2θ angle around 17° where the intensity is at the minima.

$$\%Cr = \frac{I_{002} - I_{am}}{I_{002}} \times 100 \quad (1)$$

I_{002} is the diffraction of maximum intensity caused by the nanocellulose crystalline 002 lattice peak at 2θ angle around 22°. [9, 10]

2.2 Azetidinium salts

Azetidinium salts are presented in this section. The azetidinium salts are divided into two different classes: symmetrical and asymmetrical azetidinium salts depending on the structure of their two end groups R' and R''.

2.2.1 Symmetrical azetidinium salts

The symmetrical azetidinium salts consists of a four-atom ring with a hydroxyl group at the 3'-position and two identical end groups (R' and R'') at 1,1'-nitrogen position. The nitrogen has a positive charge with chlorine as counter ion and the ring structure makes it reactive under mild conditions. The azetidinium salts have previously been shown to react with carboxylates, amines, phenols, phosphorus nucleophiles and recently also sulfate esters[5]. The azetidinium salts are sensitive to nucleophilic attack at position 2 and 4 on the ring due to the positive charge of the nitrogen and opens through a S_N2 reaction into a ring opened product. The azetidinium salts can be prepared by reaction between dialkylamines and epichlorohydrin. The reaction can form either 3-hydroxyazetidinium chloride which is the ring-closed salt or it can form the ring-open product 1-chloro-3(dialkyl amino) propan-2-ol. The reaction is unselective but the ring-closed structure is more thermodynamically favourable. The ring is however sensitive to nucleophilic attack which makes environmental factors such as solvent, temperature and presence of

nucleophiles important factors to consider when it comes to achieving the ring closed salt. The reaction can be seen in figure 3. [11, 12]

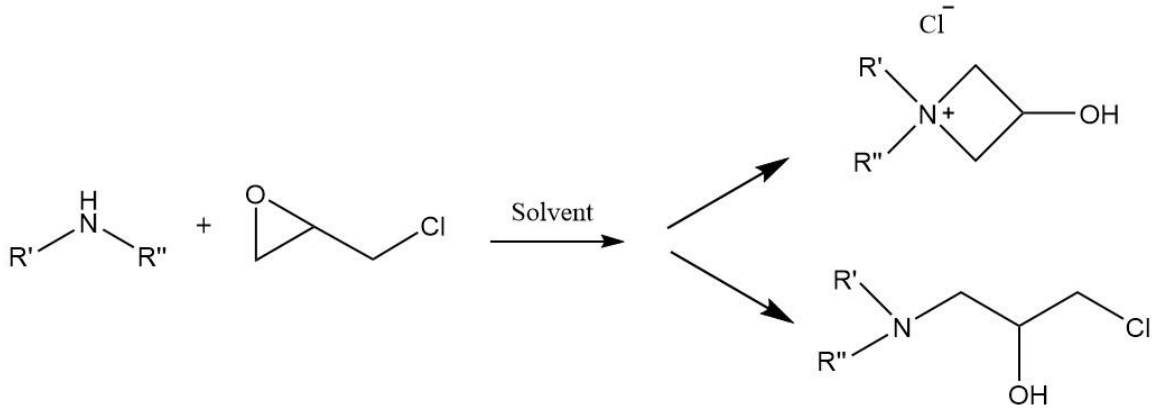

Figure 3 – Reaction between secondary amine and epichlorohydrin can result in either the ring-closed 3-hydroxyazetidinium chloride (top product) or the ring-open 1-chloro-3-amino propan-2-ol (bottom product). [13]

3-Hydroxy azetidinium chloride has a four-atom ring that can exist in two conformations. The properties will be affected depending on if the hydroxyl group is oriented in a equatorial or axial position[12]. The two conformers can be seen in figure 4.

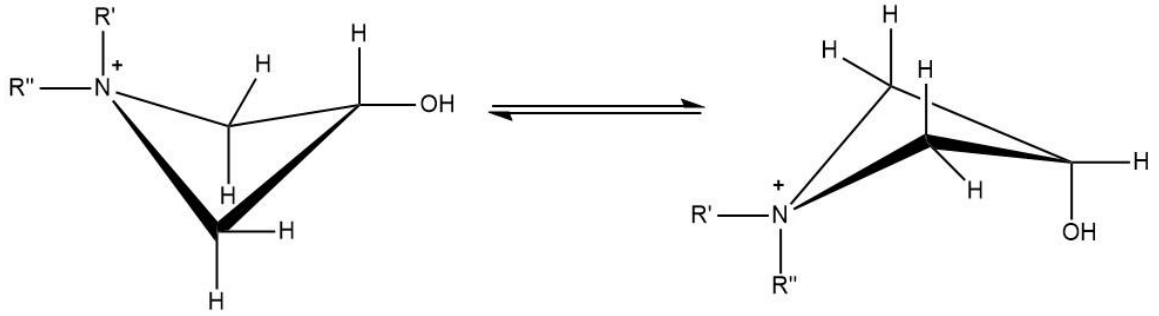

Figure 4: The two different conformational orientations of 3-hydroxy azetidinium salt. The equatorial position of the hydroxyl group in the left conformer is more stable.

It has been reported that the equatorial conformer of cyclobutane derivatives are the more stable structure of the two which would indicate that the left conformer in figure 4 is the most stable also [14].

2.2.2 Asymmetrical azetidinium salts

Asymmetrical azetidinium salts are prepared from asymmetrical secondary amines that are reacted with epichlorohydrin. Asymmetrical secondary amines have different length and/or different functional groups of the R' and R'' chains. These asymmetrical secondary amines can be prepared by reductive amination of aldehydes with primary amines under the influence of a reducing agent [15]. This reaction mechanism enables synthesis of a big variation of asymmetrical secondary amines by changing the aldehydes and primary amines used. This makes it possible to choose the R' and R'' end groups freely. The

different side groups give the possibility to give the azetidinium salts different properties and steric structure.

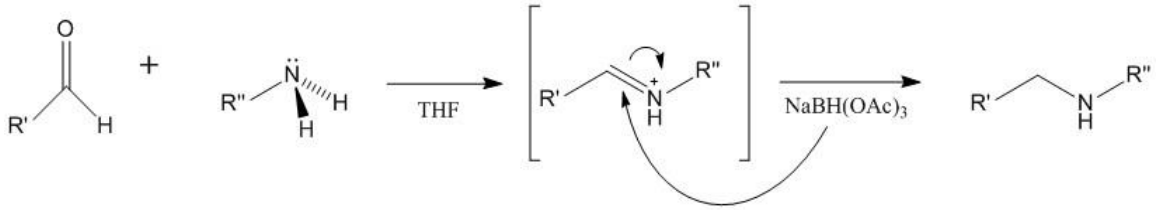

Figure 5 - Synthesis mechanism of asymmetrical secondary amines by reductive amination of aldehydes with primary amines[15].

2.3 Modification of CNC with azetidinium salts

It has previously been shown that carboxylates and sulfate esters can work as nucleophiles for ring opening of azetidinium salts. CNC reaction with azetidinium salts generates Y-shaped branching of the azetidinium salt carbon chain. This enables an alternative to more traditional ether and esterification modifications of CNC with the purpose of increasing the hydrophobicity of CNC. It's necessary to make CNC more hydrophobic for biocomposite applications. The matrix used in these composites are usually made from hydrophobic synthetic polymers. CNC has hydrophilic properties in its unmodified state and would therefore separate from the matrix without modification. Thermal properties will also improve by attaching azetidinium salts to CNC, which prevents degradation at the matrix polymers' melting temperature. Therefore it's possible to design different azetidinium salts for different CNC applications. [5] The reaction mechanism can be seen in figure 6 below.

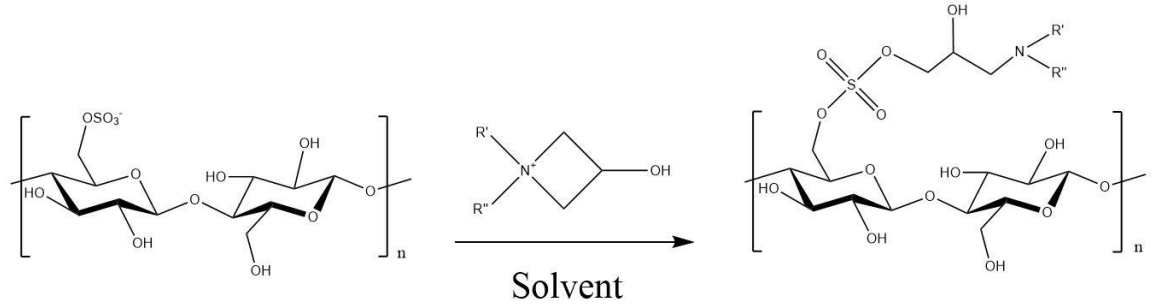

Figure 6 - Nucleophilic ring opening of azetidinium salt by reaction with sulfated CNC[5].

2.3.1 SH-functionalisation of CNC for use as electrolyte in batteries

Another new application is the possibility to produce CNC-gels with high conductivity. This type of material could potentially be used as electrolyte in lithium-ion or sodium-ion batteries for ion charge transport. The electrolytes used today contains fluorinated salts dissolved in organic liquid solvents which have raised environmental and safety concerns. Solid polymer electrolytes are much safer in these aspects but have a major drawback of low ionic conductivity. A potential solution to this could be by SH-functionalizing of CNC

modified with diallylazetidinium groups. The reactive diallyl-end group could be modified with thiol groups which can increase ionic conductivity and solve the problems generally associated with solid polymer electrolytes. Sulphur is a good atom to use since it has good ability to transport ions. Reaction mechanism can be seen in figure 7 below where thioacetic acid reacts with diallyl-modified CNC into the intermediate thioester product. This can then be reduced into the final thiol product by reduction with sodium borohydride in the presence of palladium(II) acetate catalyst. [16-18]

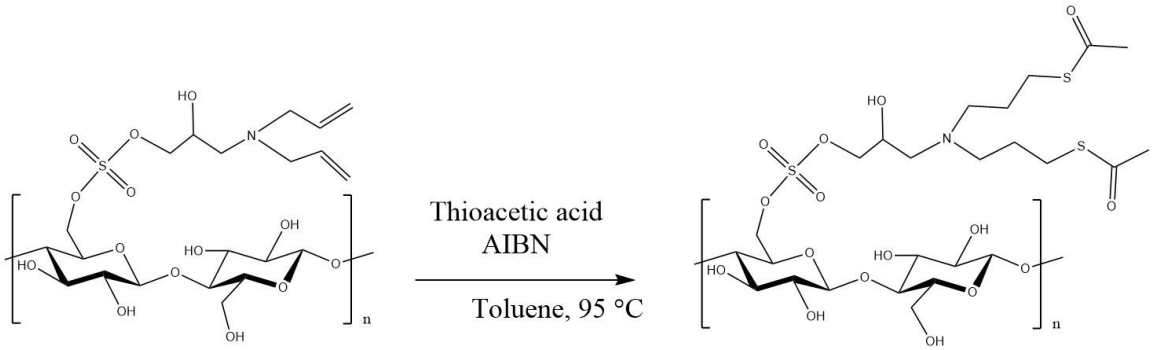

Figure 7: Reaction between allylic groups on the modified CNC with thioacetic acid.

3. Methods

The project consisted of theoretical as well as experimental parts. Literature studies were performed initially to gain knowledge on azetidinium salts, nanocrystalline cellulose, synthesis, modification and characterization procedures of these substances. Then were the experimental parts performed which consisted of synthesis and analysis of azetidinium salts and CNC.

3.1 Preparation of CNC

CNC was produced through hydrolysis of cellulose with sulfuric acid. First, cellulose was mixed with a 64 % (w/w) sulfuric acid solution. The mixture was then stirred for 2 hours at 45 °C. The reaction was then stopped by dilution in deionized water followed by centrifugation which was extended to 20 minutes at speed of 4300 rpm to achieve a solid precipitate. The supernatant was then removed and the solid re-dispersed in deionized water and re-centrifuged for a total of two times. Lastly dialysis was performed with continuous replacement of dialysis water one time every day until the conductivity dropped below 5 µS. The CNC was then re-dispersed by sonication into a colloidal suspension. [5]

3.2 Preparation of azetidinium salts

Procedure of azetidinium salt synthesis according to articles by Börjesson et al. and Chattopadhyay et al. [5, 12]. 5 mmole epichlorohydrin was added dropwise to a 5 mmole solution of secondary amine and 2 ml solvent. The solvent was varied depending on the secondary amine. Acetonitrile, isopropanol, methanol and water was used as solvents. The symmetric secondary amines used were diallylamine, bis(2-methoxyethyl)amine, dibenzylamine, morpholine and 3,3-iminodipropionitrile. Asymmetric secondary amines used were N-octylpropylamine, N-nonylpropylamine, N-undecylmethylamine, N-propargylnonylamine, N-propargylpropylamine and N-benzylpropylamine. The asymmetrical secondary amines were prepared since they were not commercially available. The temperature was varied between 0 °C, 20 °C and 40 °C during the addition to find optimal reaction conditions for some of the reactions. Generally, the mixture was stirred for 24 hours at room temperature for all reactions. The product was extracted with diethyl ether and the remaining solvent was removed in vacuum. One reaction for diallylazetidinium salt was also done on large scale where 39.8 g of epichlorohydrin was added dropwise to 42.1 g of diallylamine in 150 ml of acetonitrile at room temperature. Detailed protocol can be seen in appendix A3.

3.1 Design of experiments

The parameters chosen to alternate for the synthesis of azetidinium salts were temperature and solvents. This was done with the aim to find optimal reaction conditions for the azetidinium salts were temperature was altered for two of the salts; diallylazetidinium salt and bis(2-methoxyethyl)azetidinium salt.

The side groups of the azetidinium salts were chosen with the aim of producing salts with varying hydrophobic properties. Different amount of hydrophobic properties could be used to adjust the properties of modified CNC to match the matrix polymer in biocomposite applications. The asymmetrical salts had alkyl side groups with a total of 12 carbons but where they were shifted to 11 and 1 carbons for side groups R' and R'' for one of the salts. Another variant where done with 9 and 3 carbons long alkyl groups on R' and R''. The different carbon chain lengths will introduce different steric effects in composite applications and this could potentially be used to prevent agglomeration and improve dispersion in the matrix for example. Some other functional end-groups were also investigated such as aromatic, alkyne, nitrile, methoxy and allyl end-groups which could be used for introduction of different chemical properties.

3.3 Preparation of asymmetrical secondary amines

Asymmetrical secondary amines were prepared according to protocol by Abdel-Magid et al. [15]. Generally, an aldehyde was mixed with equimolar amount of a primary amine with THF as solvent. Sodium triacetoxyborohydride was used in 1.3 molar equivalents as reducing agent. The reaction was stirred for 24 hours under inert (N_2) atmosphere. The reaction was quenched with aqueous sodium carbonate and extracted with dichloromethane. Residual solvent was removed in vacuum. Another method by Setamdideh et al. [19] was also evaluated using a mixture of sodium borohydride and cation exchange resin as a cheaper reducing agent compared to sodium triacetoxyborohydride.

3.4 Modification of CNC with azetidinium salts

CNC should be dispersed in DMSO-toluene mixture (90:10). Azetidinium salt will then be added in equimolar amount/anhydroglucose unit and the reaction will be stirred for 22h at 90 °C. The reaction is then cooled to room temperature and washed with deionized water in repeating centrifugation steps. The final product can then be stored in solution or dried in films. [5]

3.5 Thiol-functionalisation of azetidinium modified CNC

CNC modified with diallylazetidinium salt have allyl end groups which can be functionalized with thiol groups. Generally, 10 mmol of diallylazetidinium salt or diallyl modified CNC were mixed with 70 mmol of thioacetic acid with 0.2 g of grinded 2,2′-Azobis(2-methylpropionitrile) (AIBN) as free radical initiator. Toluene was used as

solvent and the reaction was stirred over night at 95 °C in a round bottom flask equipped with a *Vigreux column* condenser. It was then centrifuged and re-dispersed in ethanol for three times. Reduction of the thioester-CNC was done by re-dispersing 1 mmol in methanol and mixing it with 3 mmol sodium borohydride as reducing agent and then add 0.05 mmol palladium (II) acetate as a catalyst.

3.5 Characterization methods and instruments

Several methods were used to characterize the synthesized azetidinium salts, unmodified CNC and the azetidinium substituted CNC. Such methods included proton nuclear magnetic resonance (H-NMR), Fourier-Transform Infrared (FTIR) spectroscopy, X-ray powder diffraction (XRD), zeta potential and atomic force microscopy (AFM). Conductivity measurements was performed with *Eutech Instruments Pte Ltd/ Oakton instruments EcoScan Con5*

3.5.1 NMR

Samples for both H-NMR and C-NMR were prepared by dissolving the samples in 0.7 ml DMSO-d_6 or $CDCl_3$ in a NMR tube. NMR analysis was conducted with *Varian 400-MR NMR Spectrometer* operating at 399.95 MHz for proton detection and 100.58 MHz for carbon detection.

3.5.2 FTIR

Samples for FTIR were prepared by mixing and 0.2 mg of sample with 300 mg of potassium bromide (KBr). The powder mixture was then pressed into tablets using a hydraulic press under vacuum. FTIR spectroscopy was performed with *PerkinElmer Spectrum One FT-IR Spectrometer* from 400 cm^{-1} to 4000 cm^{-1} using 16 accumulative scans.

3.5.3 XRD

Samples for XRD were prepared by grinding the sample into a fine powder. The powder was then added to the sample holder and was distributed with a microscope glass slide evenly. XRD was done with *Siemens D5000 Diffractometer.*

3.5.4 Zeta potential

Samples were prepared by diluting the them with milliQ-water to a concentration of 0.05%. The samples were placed in cuvettes using a syringe to prevent air bubbles from entering the cuvette. Zeta potential was then measured with *Malvern Zetasizer Nano ZS ZEN3600* at room temperature repeatedly until stable values were achieved.

3.5.5 AFM

AFM was used using tapping mode and equipped with a stiff Micro Masch silicon cantilever, with a spring constant of 40 N/m. AFM was utilized to investigate topography and size of the unmodified nanocellulose crystals. The sample was diluted 500x and a drop was placed onto a Mica sheet *(TAAB Mica Sheets M054).* AFM was performed with *Digital Instruments Santa Barbara, California Nanoscope III.*

4. Results and discussion

Results will be presented in this section for characterisation of CNC, synthesis of azetidinium salts, synthesis of asymmetrical secondary amines and modification of CNC. The raw data for the synthesized azetidinium salts and secondary amines can be found in appendix B1 and B2 respectively.

4.1 CNC characterisation

CNC was characterised with FTIR, XRD, AFM and Zeta-potential measurement. Results of powder XRD for unmodified CNC can be seen in figure 8. The percentage of crystallinity was calculated to 77,7% using equation 1 with values from figure 8. The XRD analysis confirms that the cellulose material is to a high degree crystalline.

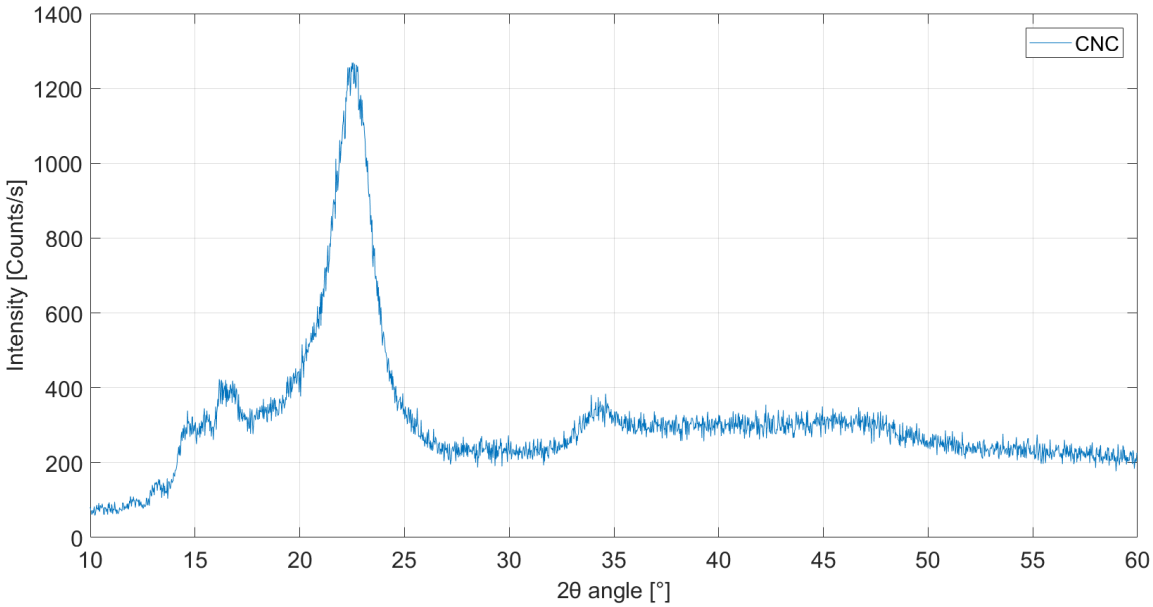

Figure 8: Diffractogram from powder XRD of unmodified CNC.

AFM was done on unmodified CNC and the variation of size of the nanocrystals can be seen in table 1. The results show that nanocrystals have formed during the treatment with sulfuric acid.

Table 1: Size interval from AFM of cellulose nanocrystals. Smallest and biggest length and diameter values measured for the sample nanocrystals.

	Minimum (nm)	**Maximum (nm)**
Crystal length	160	235
Crystal diameter	4,8	6,2

AFM image of the nanocellulose crystals can be seen in figure 9.

Figure 9: AFM image of cellulose nanocrystals

4.2 Characterisation of modified CNC

FTIR was done on pure CNC, CNC modified with diallylazetidinium salt and thioester functionalised diallylazetidinium-CNC as well as the reduced thiol-CNC. Results can be seen in figure 10 where peak at 1740 cm^{-1} the oven dried thioacetate modified sample show a carbonyl peak (C=O). The oven-dried sample also shows reduction of water as can be seen by the disappearance of the water peak at 1640 cm^{-1} compared to the airdried sample. The peak at 3400 cm^{-1} has also narrowed down for the oven dried sample which indicates loss of water. The marked peak at 815 cm^{-1} is an indication of that diallylazetidinium salt has attached to the sulfate groups on CNC. The peak belongs to the C-O-S group and the shift in wavenumbers to 800 for the modified sample indicates that the sulfate group has reacted with the salt[20]. The peak at 1740 cm^{-1} for the oven-dried sample indicates presence of thioester groups on the CNC. In the thiol-CNC samples it can be seen that this peak has disappeared which indicates that the thioester has been reduced into the thiol. The thiol group S-H stretch vibrations should be visible at around 2500 cm^{-1} in theory but due to low degree of modification this peak can be difficult to observe. [21, 22]

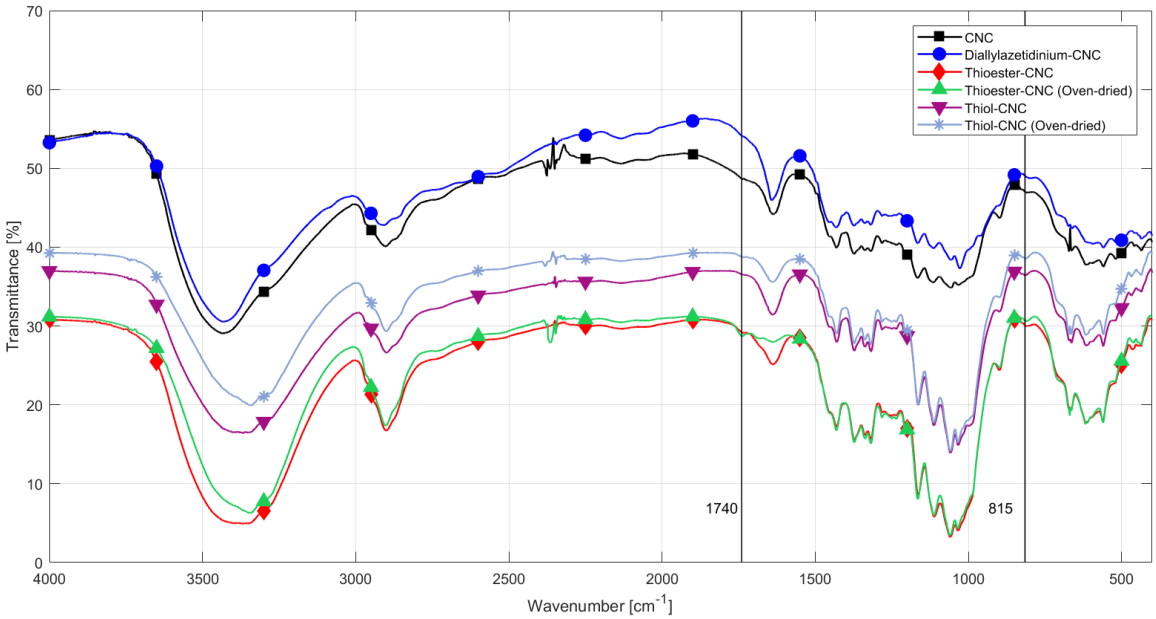

Figure 10: FTIR spectra of unmodified CNC, diallylazetidinium modified CNC, thioester functionalised CNC, oven-dried thioester functionalised CNC, thiol-CNC and oven-dried thiol-CNC.

Zeta (ζ) potential was measured for both unmodified CNC and for CNC modified with diallylazetidinium salt. The modified CNC shows a lower zeta potential compared to the unmodified CNC indicating successful modification. Results can be seen in table 2.

Table 2: Results from zeta potential measurement of unmodified CNC and CNC modified with diallylazetidinium salt.

Sample	**ζ-potential (mV)**
CNC	-48,7
CNC-diallylazetidinium	-32,3

4.3 Results from synthesis of azetidinium salts

Azetidinium salts were synthesized during different reaction conditions where temperature and solvent where varied. NMR was used to identify the most promising reaction conditions. The success of the reactions was graded a score between 0 and 5 where 0 meant no product and a score of 5 meant pure product without any starting material left. Results for synthesis of azetidinium salts can be seen in table 3. Reactions in acetonitrile and isopropanol worked best at room temperature compared to reactions conducted at 0 °C. Reactions at 40 °C worked slightly better but best results was achieved at room temperature. Problems with overlapping peaks made it difficult to calculate exact yields for the azetidinium salts and therefore a quantitative grading was used instead.

Table 3: List of the synthesis parameters for the different azetidinium salts evaluated and results from synthesis the salts. R1 and R2 are the side-groups on the azetidinium salts.

Number	R1	R2	Open form	Ring-closed form	Solvent	Temperature (°C)
1	Morpholine	Morpholine	0	4	Methanol	0
6	Allyl	Allyl	0	0	Acetonitrile	0
2	Allyl	Allyl	0	5	Acetonitrile	20
3	Allyl	Allyl	0	3	Isopropanol	20
8	Allyl	Allyl	0	2	Acetonitrile	40
9	Allyl	Allyl	2	2	Isopropanol	40
7	Methoxyethyl	Methoxyethyl	3	1	Isopropanol	0
4	Methoxyethyl	Methoxyethyl	0	0	Acetonitrile	20
5	Methoxyethyl	Methoxyethyl	1	4	Isopropanol	20
10	Methoxyethyl	Methoxyethyl	1	1	Acetonitrile	40
11	Methoxyethyl	Methoxyethyl	1	1	Isopropanol	40
12	Propionitrile	Propionitrile	3	0	Water	20
13	Propionitrile	Propionitrile	3	0	Isopropanol	20
14	Propionitrile	Propionitrile	1	0	Acetonitrile	20
15	Nonyl	Propyl	1	0	Acetonitrile	20
16	Nonyl	Propyl	1	3	Isopropanol	20
17	Undecyl	Methyl	1	1	Acetonitrile	20
18	Undecyl	Methyl	0	1	Isopropanol	20
19	Benzyl	Benzyl	4	0	Acetonitrile	20

20	Benzyl	Benzyl	4	0	Isopropanol	20
21	Benzyl	Benzyl	1	0	Water	20
22	Nonyl	Propargyl	0	0	Acetonitrile	20
23	Nonyl	Propargyl	0	2	Isopropanol	20

A NMR spectra will be given as an example and can be seen in figure 11 for diallylazetidinium salt (2). The hydroxyl peak is characteristic for the ring-closed azetidinium salts and usually appear between 6-7 ppm with little overlapping from other signals. Other significant peaks are the signals for the hydrogens on carbon 1, 2 and 4 in the ring which usually appear at around 4-5 ppm. A upfield shift in peaks would be a strong indication of a ring-open product together with a shift upfield for the hydroxyl group. NMR data confirmed that the ring-closed product 3 was formed. ^{1}H-NMR (400 MHz, DMSO-d_6) δ 6.69 (ddd, J = 7.3, 2.7, 1.4 Hz, 1H), 6.05 – 5.90 (m, 2H), 5.72 – 5.54 (m, 6H), 4.67 – 4.54 (m, 1H), 4.48 – 4.38 (m, 2H), 4.30 – 4.18 (m, 2H), 4.14 – 4.07 (m, 2H), 3.94 (d, J = 7.1 Hz, 2H)

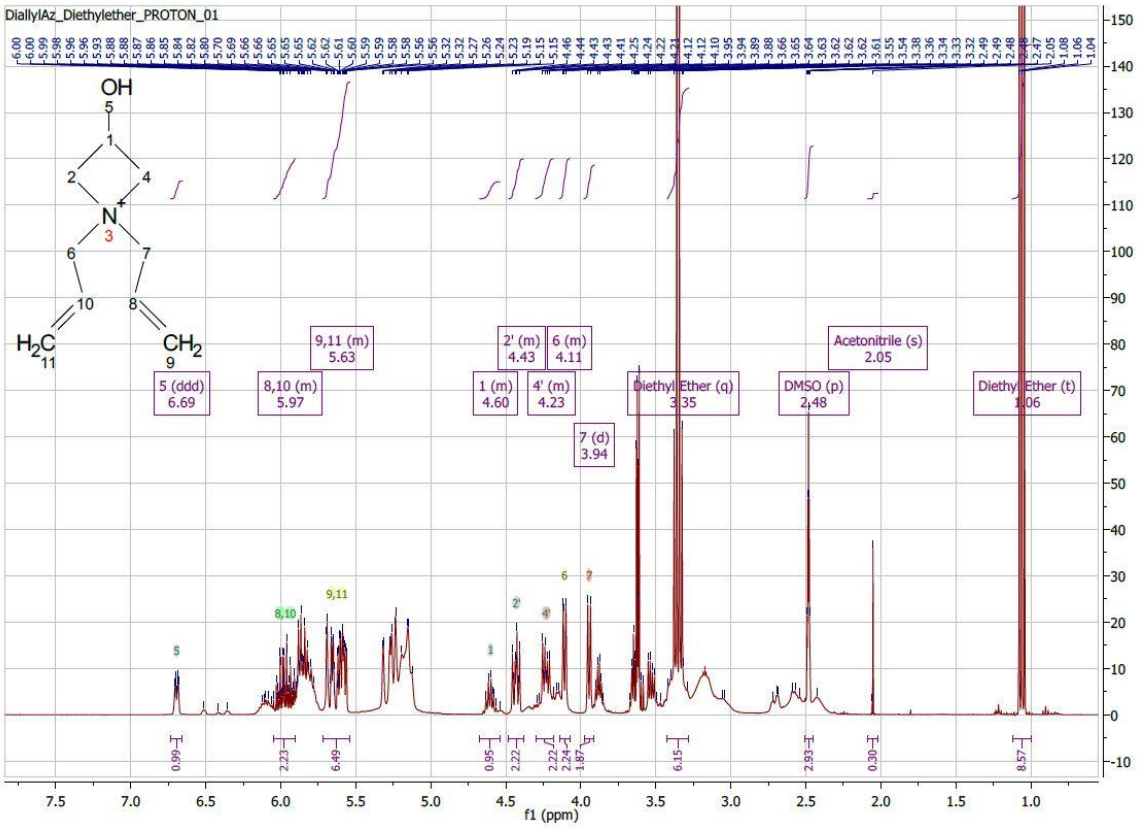

Figure 11: NMR spectra of product 3 diallylazetidinium salt synthesised at room temperature with acetonitrile as solvent.

Raw NMR data for the other azetidinium salts can be seen in appendix B1. The results show that there isn't any general synthesis pathway that works for all azetidinium salts. Variations in polarity and steric structure could influence the results and different solvents have worked differently well. The reactions in both acetonitrile and isopropanol have both resulted ring-closed and ring-open products. No apparent pattern could be observed for which reaction conditions that are optimal for the synthesis of azetidinium salts. Instead, it seemed to depend from salt to salt.

4.4 Results from synthesized secondary amines

The synthesized secondary amines where verified with ^{1}H-NMR spectroscopy. In general, the reductive amination with sodium triacetoxyborohydride (STAB) worked well. The synthesis with sodium borohydride resulted in low yield of product but could potentially work for other amines. The synthesis of the same amine with STAB gave also quite poor result which could indicate some other problems in the reaction apart from the reducing agent used. Results can be seen in table 4 for the synthesized amines. Raw data can be seen in appendix B2.

Table 4: List of synthesized asymmetric secondary amines.

R1-NH2	R2-CHO	Secondary amine	Reducing agent
Benzylamine	Propanal	4	STAB
Octylamine	Propanal	4	STAB
Propylamine	Nonanal	5	STAB
Methylamine	Undecanal	4	STAB
Propargylamine	Propanal	1	NaBH4/Dowex
Propargylamine	Propanal	2	STAB
Propargylamine	Nonanal	4	STAB

5. Conclusions

Microfibrillated cellulose was successfully transformed into sulfated nanocrystalline cellulose with nanocrystals with lengths around 200 nm and widths of about 5 nm in diameter.

Synthesis of symmetrical and asymmetrical azetidinium salts varied in success. As can be seen in table 3, the tested synthesis conditions gave wide variety of different results. Generally, the reactions worked best at room temperature but the solvent used needs to be optimized for each azetidinium salt depending on the side groups properties. The solvents used in this study, acetonitrile and isopropanol shows that some of the reactions are possible to carry out under mild conditions.

The synthesis of asymmetric secondary amines worked well using sodium triacetoxyborohydride as reducing agent for reductive amination of the aldehydes except for propargylpropylamine which had low boiling point due to short side chains and evaporated during synthesis. Sodium borohydride/Dowex didn't perform as good as expected. It could be noted that the same reaction didn't work flawlessly for the sodium triacetoxyborohydride either. The drawback of using sodium borohydride is that it's not selective and it reduces the aldehyde into alcohol instead of forming the imine in the absence of cation exchange resin. This method could if improved be a cheaper alternative compared to using the more expensive sodium triacetoxyborohydride.

Modification of CNC was confirmed by zeta potential measurement and FTIR. As can be seen in figure 10, diallyl-modified CNC show a shift at 815 cm^{-1} compared to the reference CNC sample which indicates that sulfate groups on the CNC has reacted with the diallylazetidinium salt successfully. This modified was also functionalised by attachment of thiol groups with intention for possible battery applications. As can be seen in figure 10, the peak for thioester functional group at 1740 cm^{-1} has disappeared after reduction with palladium acetate catalyst and sodium borohydride. This is an indication that the thioester has been reduced into the desired thiol-group.

Future work can lead to several new applications for the azetidinium salts. It's been shown that azetidinium salts improve thermal properties of CNC after modification. If it's possible to find mild reaction conditions without the use of DMSO as solvent that works for the modification of CNC with azetidinium salts, they could be used in future biocomposite material applications. Possible uses could be in designing degradable biocomposite plastics for example. Other future applications could be in pharmaceutical applications where the modified CNC could work as an excipient for controlled drug release. A schematic illustration of how the azetidinium salts can be utilized for different applications can be

seen in figure 12. The thiol-functionalization of CNC needs to be investigated further but could potentially be used as the future's solid polymer electrolyte in sodium batteries.

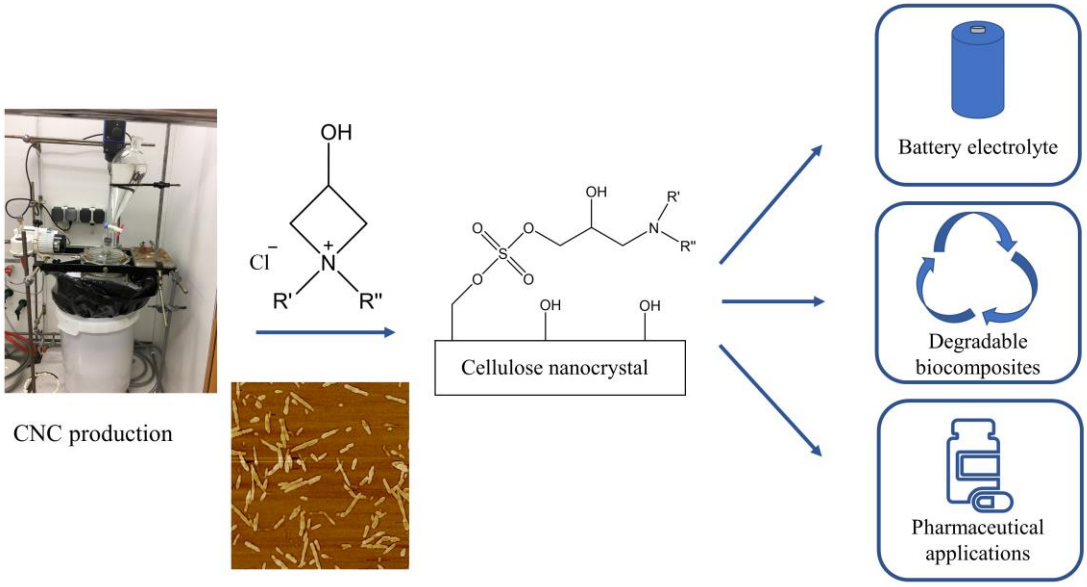

Figure 12: Illustration of how CNC can be modified with azetidinium salts and used in different applications.

6. References

1. John, M.J. and S. Thomas, *Biofibres and biocomposites.* Carbohydrate Polymers, 2008. **71**(3): p. 343-364.
2. Smole, M., et al., *Plant fibres for textile and technical applications.* Advances in Agrophysical Research, 2013. **10**: p. 52372.
3. Percival, E.G.V., *Carbohydrate sulphates.* Quarterly Reviews, Chemical Society, 1949. **3**(4): p. 369-384.
4. Gårdebjer, S., et al., *Using Hansen solubility parameters to predict the dispersion of nano-particles in polymeric films.* POLYMER CHEMISTRY, 2016. **7**(9): p. 1756-1764.
5. Börjesson, M., *Chemical modification of polysaccharides: fundamental research with an applied perspective*. 2016, Chalmers University of Technology: Göteborg.
6. Glick, B.R., J.J. Pasternak, and C.L. Patten, *Molecular biotechnology: principles and applications of recombinant DNA*. 4th ed. 2010, Washington, DC: ASM Press.
7. Brady, G.S., et al., *Materials handbook : an encyclopedia for managers, technical professionals, purchasing and production managers, technicians, and supervisors*. 2002, New York: McGraw-Hill.
8. Dufresne, A., C. Ebook, and Knovel, *Nanocellulose: from nature to high performance tailored materials*. 1. Aufl. ed. 2012, Berlin;Boston;: De Gruyter.
9. Maiti, S., et al., *Preparation and characterization of nano-cellulose with new shape from different precursor.* CARBOHYDRATE POLYMERS, 2013. **98**(1): p. 562-567.
10. Morais, J.P.S., et al., *Extraction and characterization of nanocellulose structures from raw cotton linter.* Carbohydrate Polymers, 2013. **91**(1): p. 229-235.
11. Drouillat, B., et al., *Insight into the regioselectivity of nucleophilic ring-opening of azetidinium ions containing quaternary carbon atoms.* European Journal of Organic Chemistry, 2012. **2012**(30): p. 6005-6012.
12. Chattopadhyay, S., H. Keul, and M. Moeller, *Functional Polymers Bearing Reactive Azetidinium Groups: Synthesis and Characterization.* Macromolecular Chemistry and Physics, 2012. **213**(5): p. 500-512.
13. Ross, J.H., D. Baker, and A.T. Coscia, *Some reactions of epichlorohydrin with amines.* Journal of Organic Chemistry, 1964. **29**(4): p. 824-826.
14. Berg, U., *Stereochemical Aspects—Conformation and Configuration*, in *The Chemistry of Cyclobutanes*. 2006, John Wiley & Sons, Ltd. p. 83-131.
15. Abdel-Magid, A.F., et al., *Reductive amination of aldehydes and ketones with sodium triacetoxyborohydride. Studies on direct and indirect reductive amination procedures.* Journal of Organic Chemistry, 1996. **61**(11): p. 3849-3862.
16. Boschin, A., et al., *Sodium batteries: from liquid to polymer electrolytes*. 2016, Chalmers University of Technology: Göteborg.
17. Camerano, J.A., et al., *Peripheral SH-functionalisation of carbosilane dendrimers including the synthesis of the model compound*

dimethylbis(propanethiol)silane and their interaction with rhodium complexes. Dalton Transactions, 2005(18): p. 3092-3100.
18. Choi, J., et al., *Synthesis of thiols via palladium catalyzed methanolysis of thioacetates with borohydride exchange resin.* Synthetic Communications, 1995. **25**(17): p. 2655-2663.
19. Setamdideh, D. and F. Sepehraddin, *Convenient Reductive Amination of Aldehydes by NaBH4/Cation Exchange Resin.* JOURNAL OF THE MEXICAN CHEMICAL SOCIETY, 2014. **58**(1): p. 22-26.
20. Chen, G., et al., *Improved process for the production of cellulose sulfate using sulfuric acid/ethanol solution.* Carbohydrate Polymers, 2013. **95**(1): p. 332-337.
21. Pavia, D.L., *Introduction to spectroscopy*. 5th ed. 2015, Stamford, CT: Cengage Learning.
22. Huang, J.L., C.J. Li, and D.G. Gray, *Functionalization of cellulose nanocrystal films via "thiol-ene" click reaction.* RSC ADVANCES, 2014. **4**(14): p. 6965-6969.

Appendix

Appendix A - Protocols

A1 - FTIR protocol

1. Mix 2 mg of sample with 300 mg KBr and grind into a fine powder.
2. Then use hydraulic press to form tablet from the sample powder. Setup of press according to figure 13 below. Apply vacuum for 2 minutes and then close the valve and pump up 8 tons of pressure. Maintain pressure for 1 minute and the release it slowly. Remove vacuum and turn cylinder upside down to remove tablet slowly.

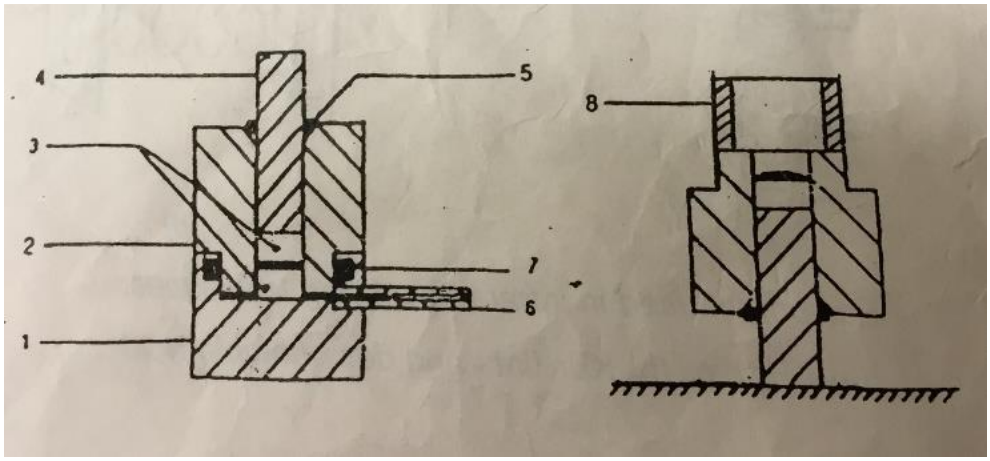

Figure 13: Set-up of tablet press sample holder.

3. Start FTIR instrument and perform background scan without sample.
4. Place tablet in FTIR instrument and perform scan from 4000 cm^{-1} to 400 cm^{-1}

A2 - NMR protocol

1. Add 5 mg of sample into a NMR tube.
2. Add 0,7 ml DMSO-d_6 into the tube and then put a cap on the tube to seal it.
3. Turn the tube upside down to mix sample and solvent thoroughly.
4. Label tube and run NMR instrument.

A3 - Protocol for synthesis of N,N-dialkylazetidinium salt

Reaction occur according to figure 14.

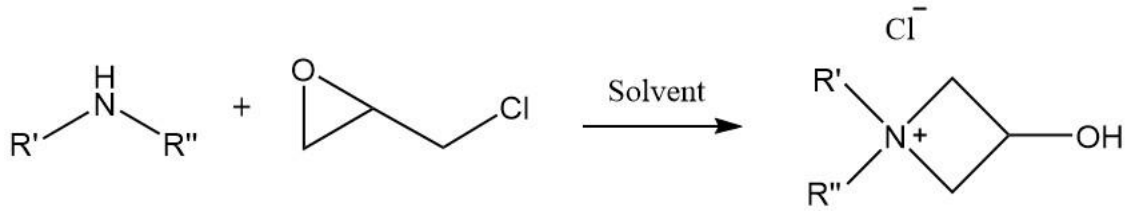

Figure 14 - Reaction between epichlorohydrin and secondary amine in solvent which forms azetidinium salt

1. In general, 5 mmol dialkylamine was mixed with 2 ml solvent (acetonitrile or isopropanol).
2. The equivalent amount of epichlorohydrin (5 mmol) was added dropwise into the solution due to exothermic reaction.
3. The reaction is then allowed to stir for 24 h at room temperature.
4. The remaining solvent is then removed in vacuum.

Protocol for the synthesis of asymmetric secondary amines by reductive amination
Reaction occurred according to figure 15.

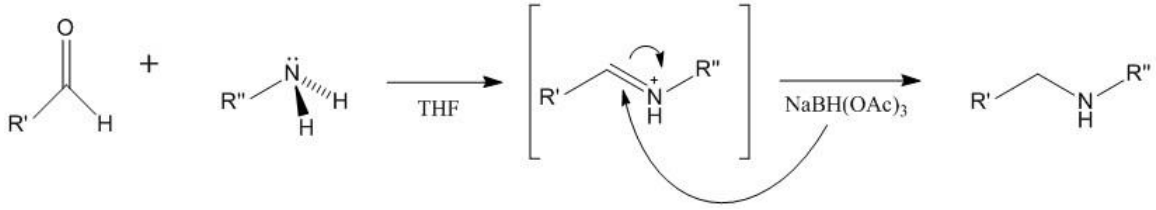

Figure 15 - Reductive amination of an aldehyde

1. 5 mmol of aldehyde and 15 ml of tetrahydrofuran was mixed in a round bottom flask.
2. 5 mmol of primary amine was added to the flask.
3. A reducing agent (sodium triacetoxyborohydride) was added in 1,4 mol equivalents
4. The reaction was stirred for 2 hours in nitrogen atmosphere.
5. The reaction was quenched by addition of aquous $NaHCO_3$ and then extracted with dichloromethane.
6. The solvents where removed in vacuum.

A4 - Protocol for XRD

XRD can be performed on powder samples as well as film samples

Powder protocol

1. Grind sample into a fine powder with a mortar and pestle
2. Add powder to sample holder. The sample should cover an area of 1x1 cm of the center part of the sample holder.
3. Use a microscope glass slide to press sample even onto the sample holder
4. Confirm that the X-ray shutter is closed in the instrument. Place the sample holder in the instrument from below. Close doors to instrument carefully.
5. Run instrument.

Film protocol

1. Add reusable adhesive onto sample holder. Screw sample holder into desired height at 1-2 mm below the reference height depending on film thickness.
2. Add sample film onto adhesive and use press with aluminum foil on top of the sample film, to prevent contamination of the sample, and press sample in place. Remove aluminum foil from sample.
3. Confirm that the X-ray shutter is closed in the instrument. Place the sample holder in the instrument from below. Close doors to instrument carefully.
4. Run instrument.

Appendix B – Results

B1 – Azetidinium salts

In this section will results from 1H-NMR be presented for the azetidinium salts in table

B1.1 Morpholineazetidinium salt

The chemical structure is shown in figure 16 for morpholineazetidinium salt.

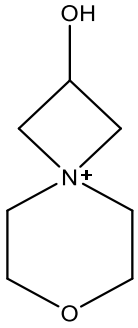

Figure 16: Chemical structire of morpholineazetidinium salt

^{1}H-NMR spectra for product 1 is shown in figure 17.

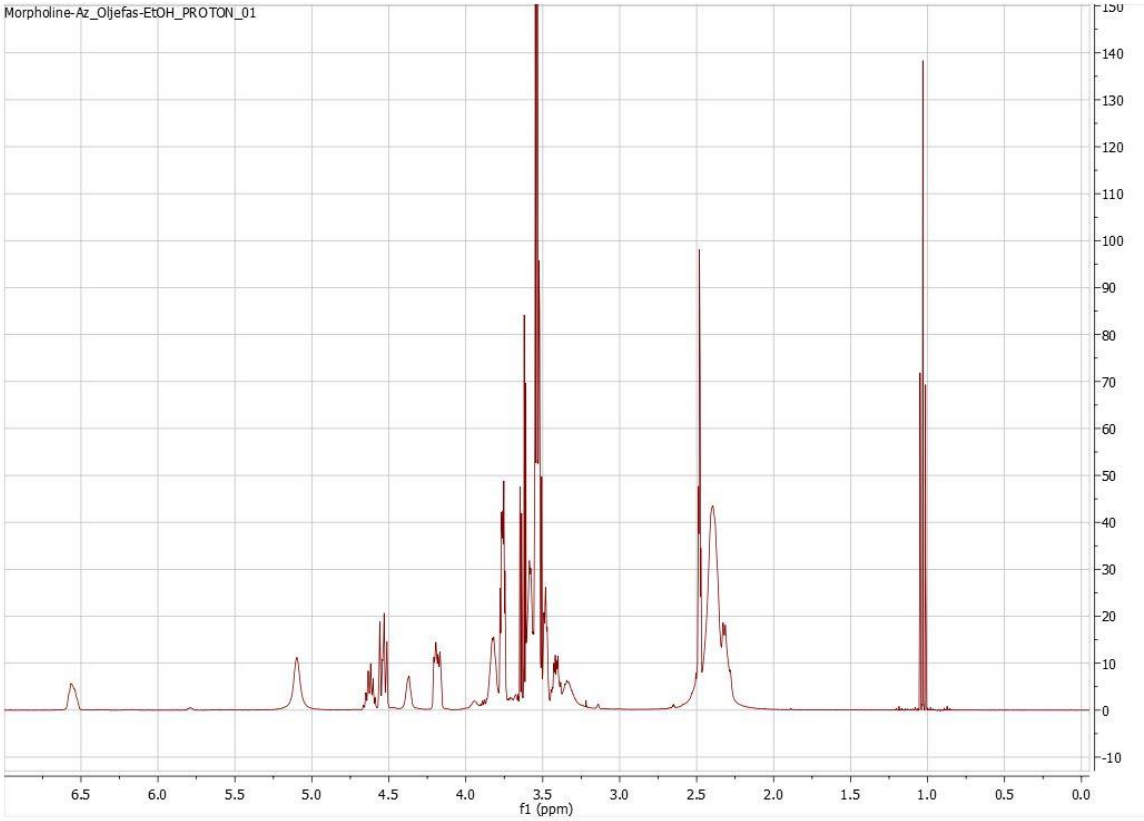

Figure 17: ^{1}H-NMR spectrum for product 1.

B1.2 Diallylazetidinium salt

The chemical structure for diallylazetidinium salt is shown in figure 18.

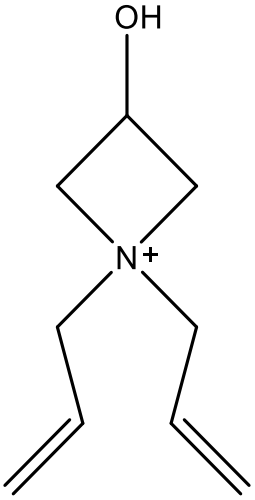

Figure 18: Chemical structure of diallylazetidinium salt

^{1}H-NMR spectra for product 2, 3, 4, 5 and 6 are shown in figure 19, 20, 21, 22 and 23 respectively.

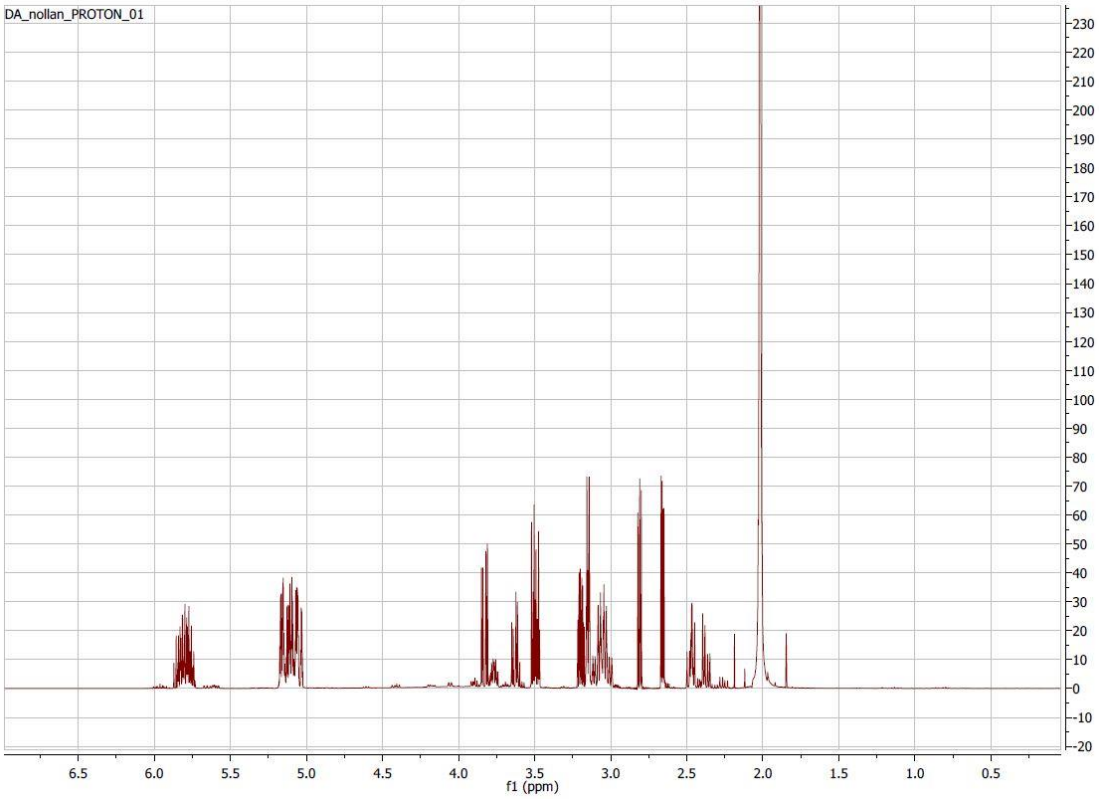

Figure 19: ^{1}H-NMR spectrum of product 2.

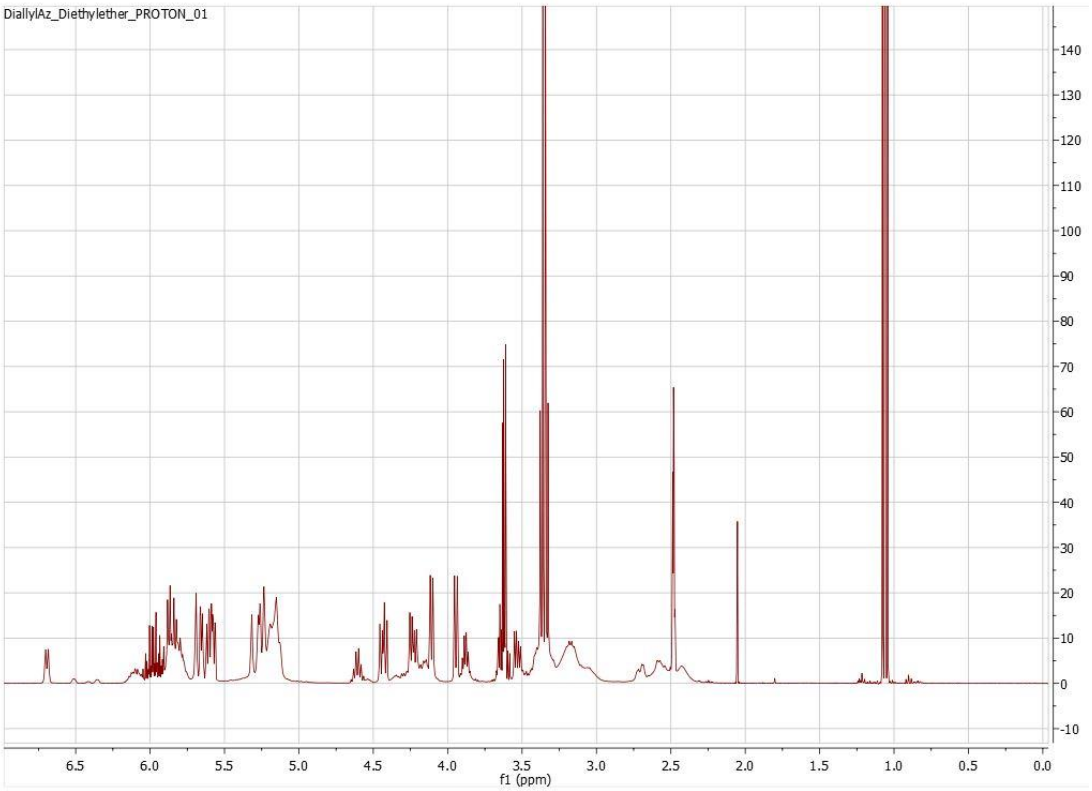

Figure 20: [1]H-NMR spectrum of product 3.

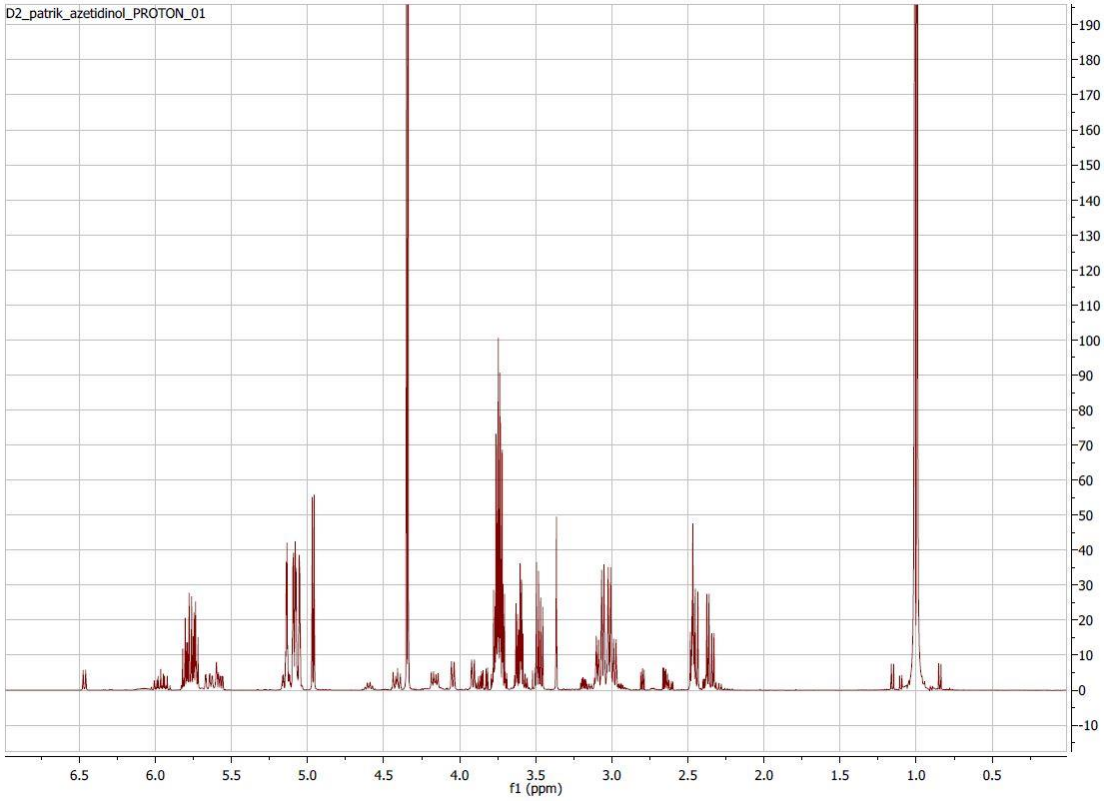

Figure 21: [1]H-NMR spectrum of product 4.

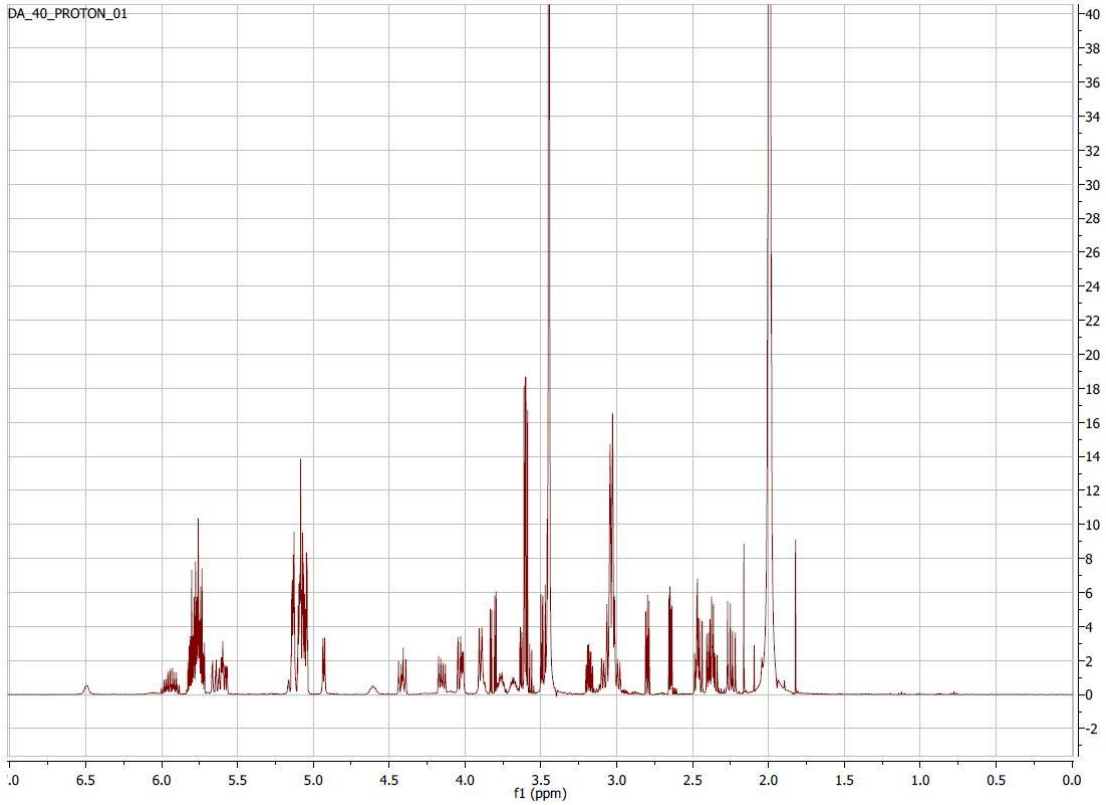

Figure 22: [1]H-NMR spectrum of product 5

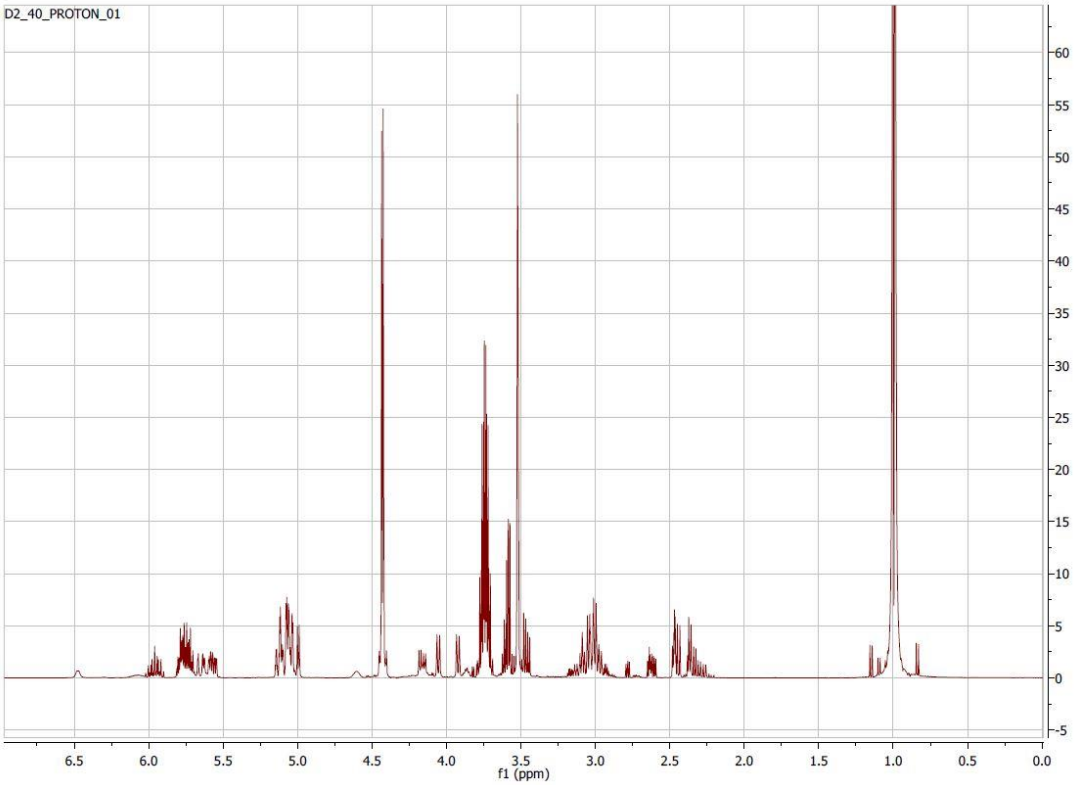

Figure 23: [1]H-NMR spectrum of product 6.

B1.3 Bis(2-methoxyethyl)azetidinium salt

The chemical structure for bis(2-methoxyethyl)azetidinium salt is shown in figure 24.

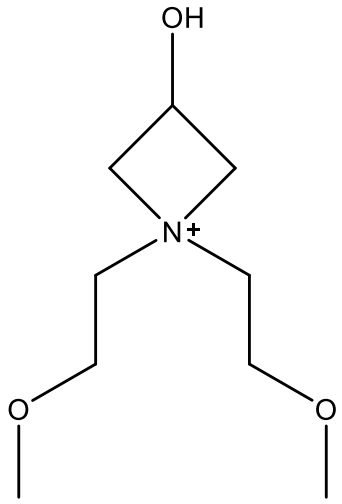

Figure 24: Chemical structure of bis(2-methoxyethyl)azetidinium salt

1H-NMR spectra are shown for product 7, 8, 9, 10 and 11 in figure 25, 26, 27, 28 and 29 respectively.

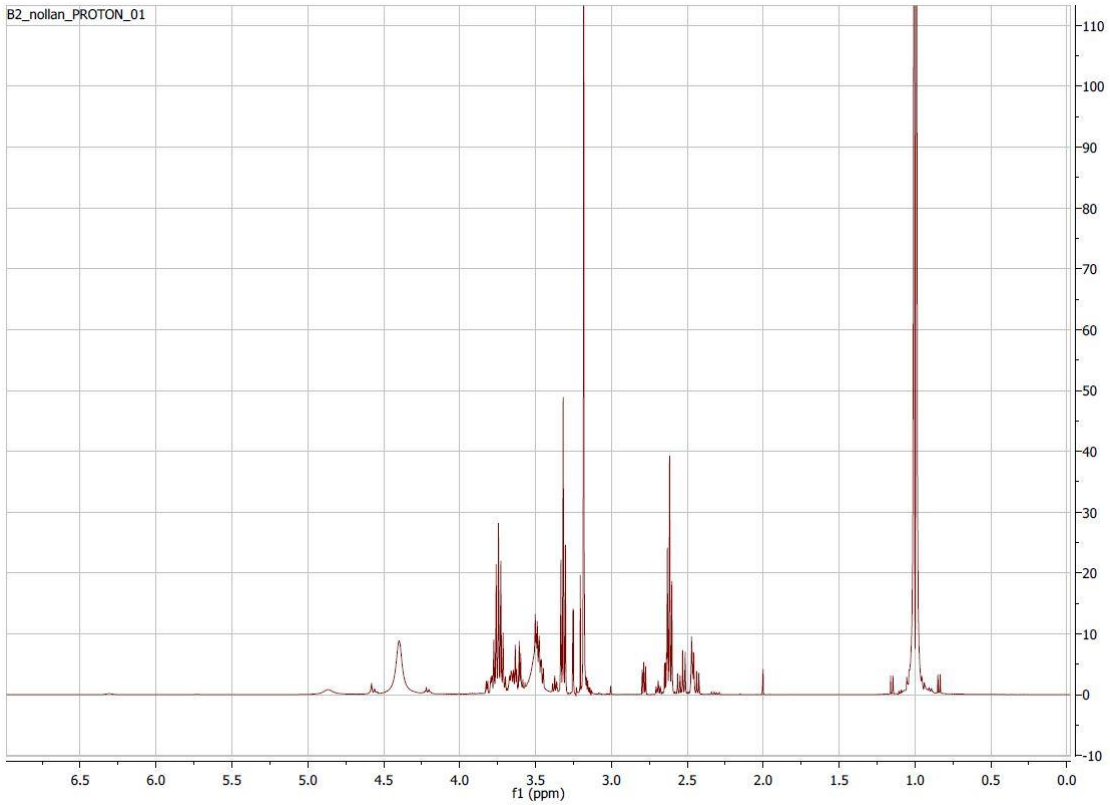

Figure 25: ^{1}H-NMR spectrum of product 7.

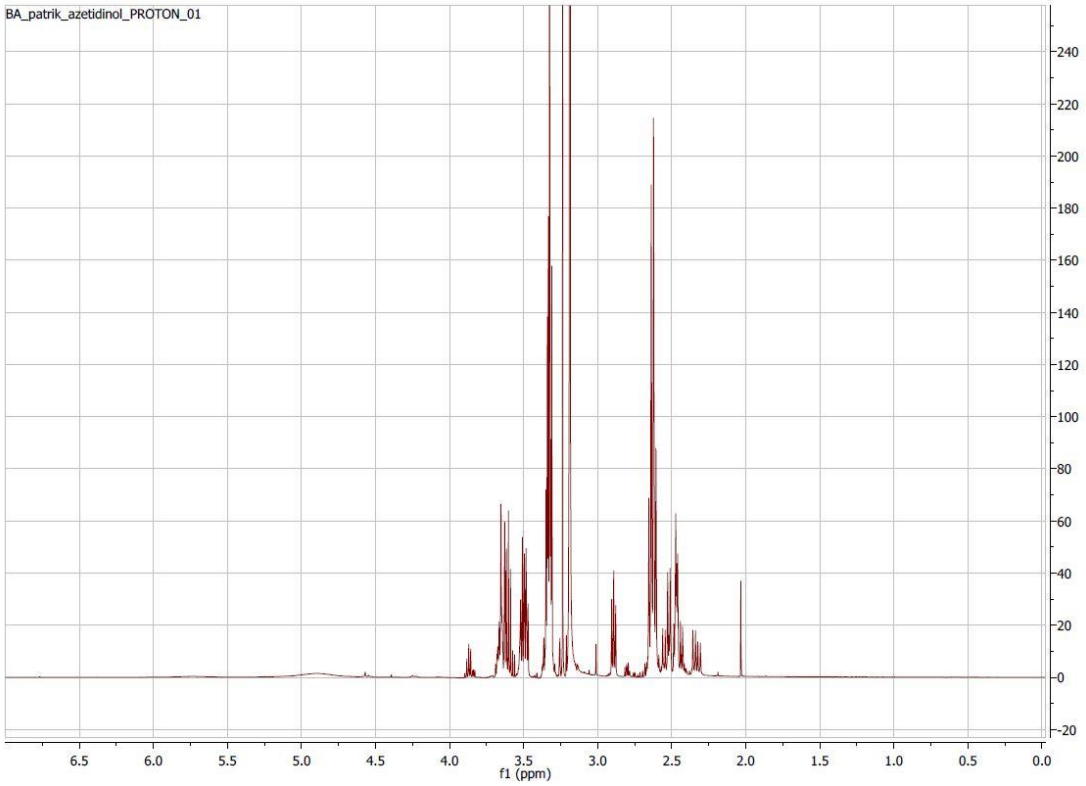

Figure 26: [1]H-NMR spectrum of product 8.

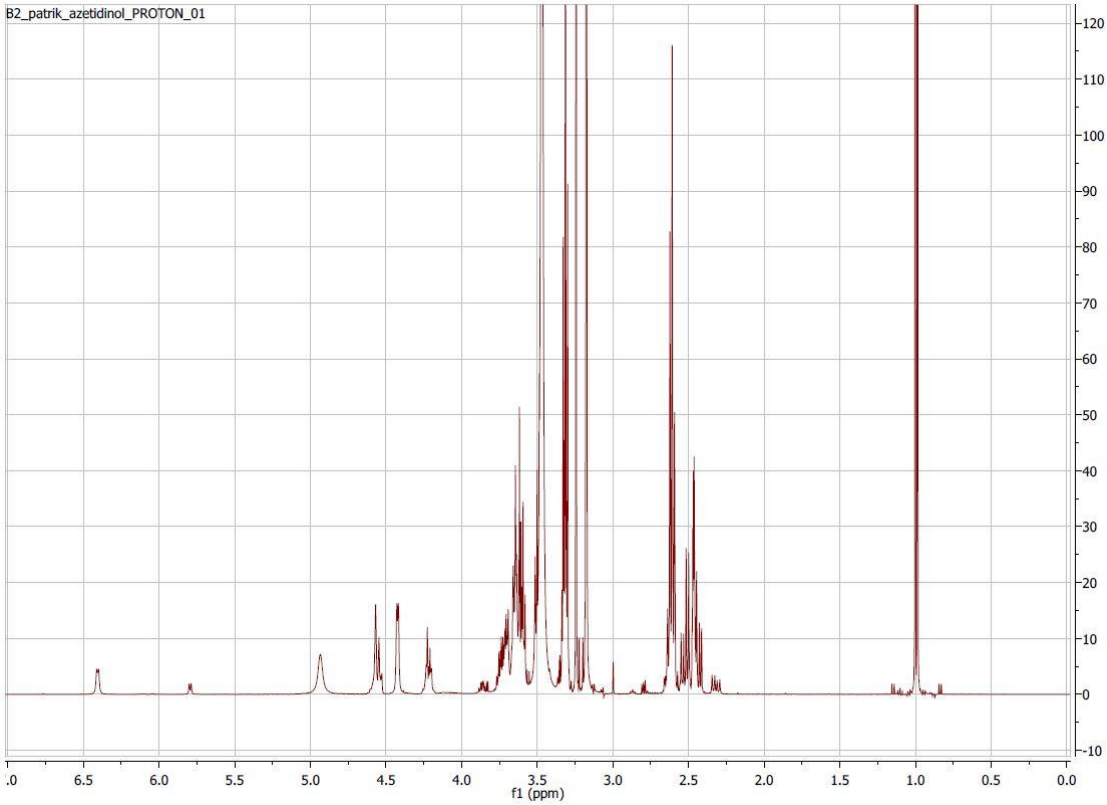

Figure 27: [1]H-NMR spectrum of product 9.

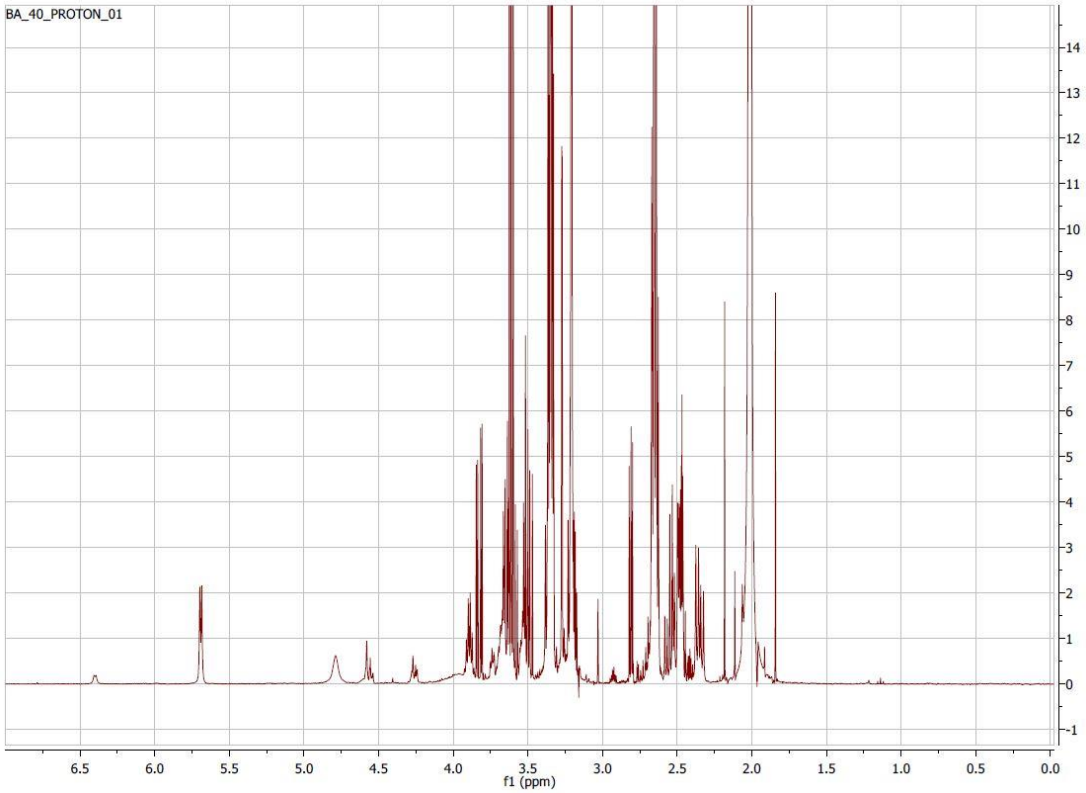

Figure 28: ^{1}H-NMR spectrum of product 10.

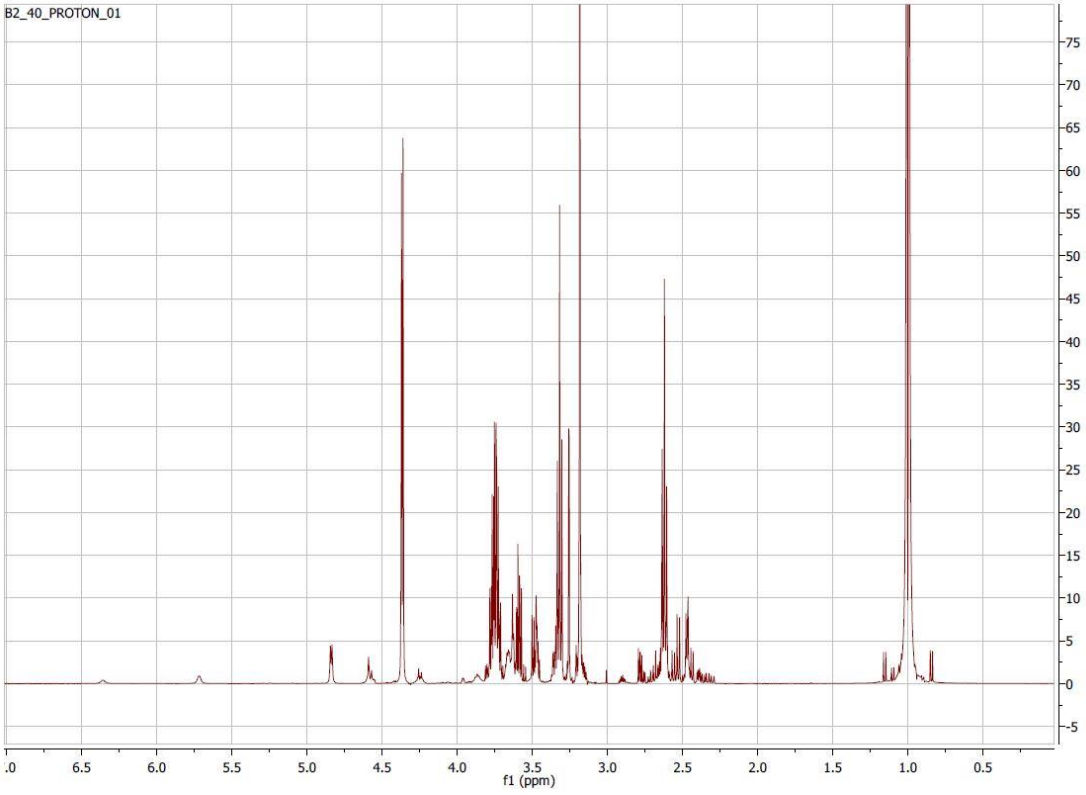

Figure 29: ^{1}H-NMR spectrum of product 11.

B1.4 3,3'-Iminodipropionitrileazetidinium salt

The chemical structure 3,3'-Iminodipropionitrileazetidinium salt is shown in figure 30.

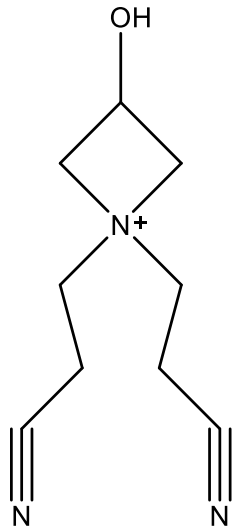

Figure 30: Chemical structure of 3,3'-Iminodipropionitrileazetidinium salt

^{1}H-NMR spectra for product 13, 14 and 15 are shown in figure 31, 32 and 33 respectively.

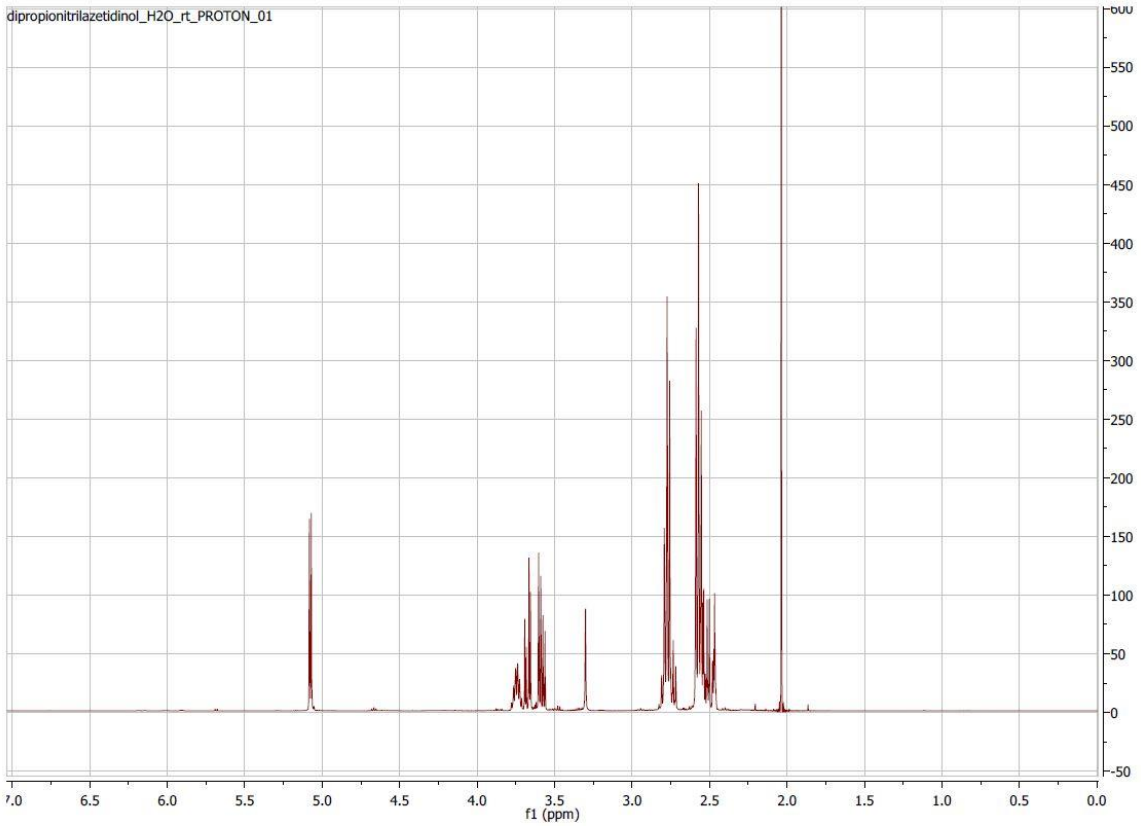

Figure 31: ^{1}H-NMR spectrum for product 12.

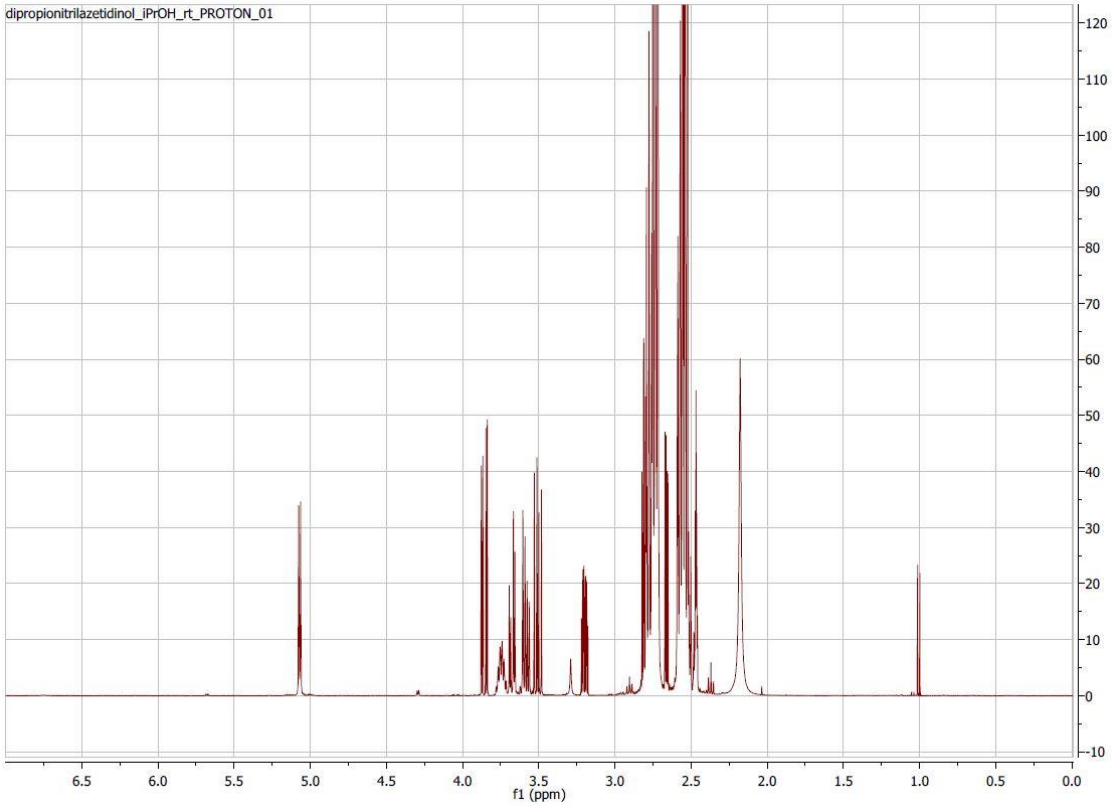

Figure 32: [1]H-NMR spectrum for product 13.

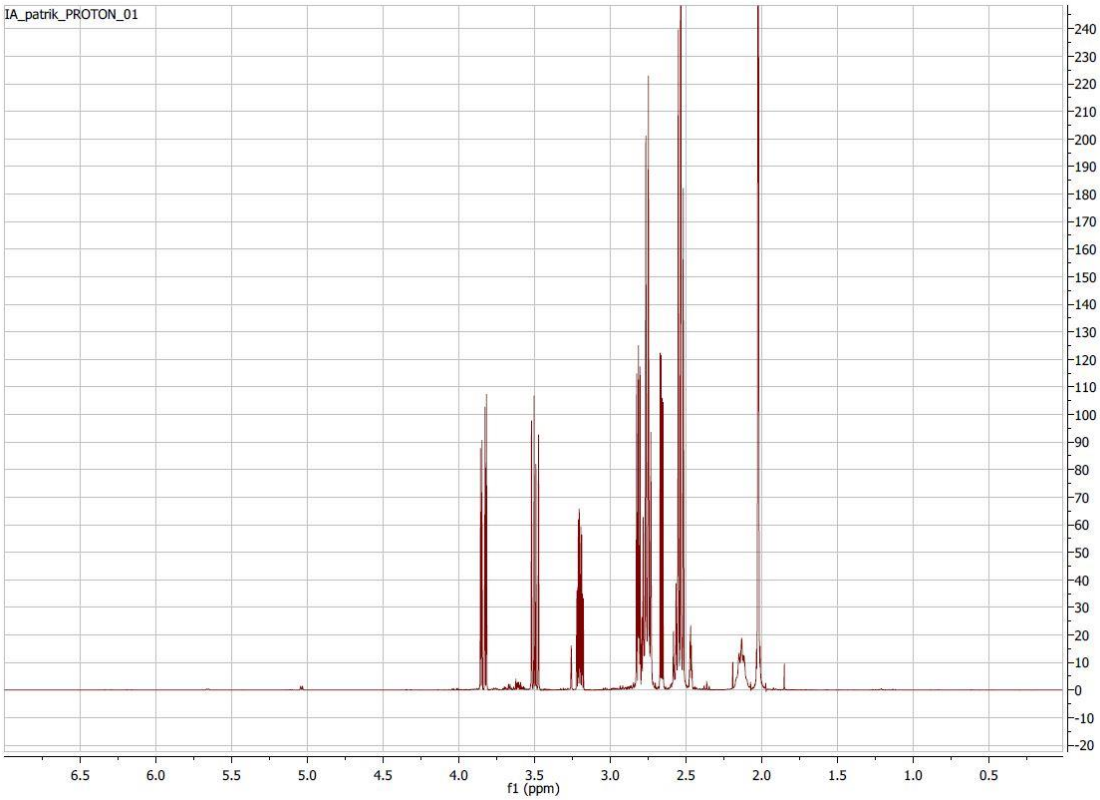

Figure 33: [1]H-NMR spectrum for product 14.

B1.5 Nonylpropylazetidinium salt

The chemical structure of nonylpropylazetidinium salt is shown in figure 34.

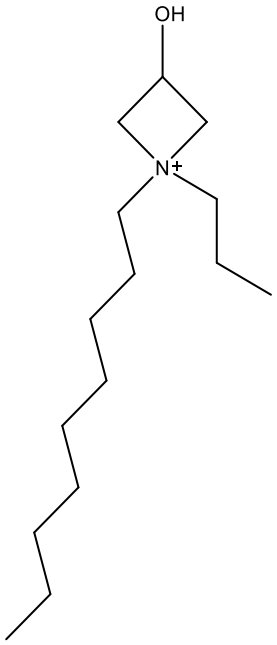

Figure 34: Chemical structure of nonylpropylazetidinium salt.

1H-NMR spectra for product 15 and 16 are shown in figure 35 and 36 respectively.

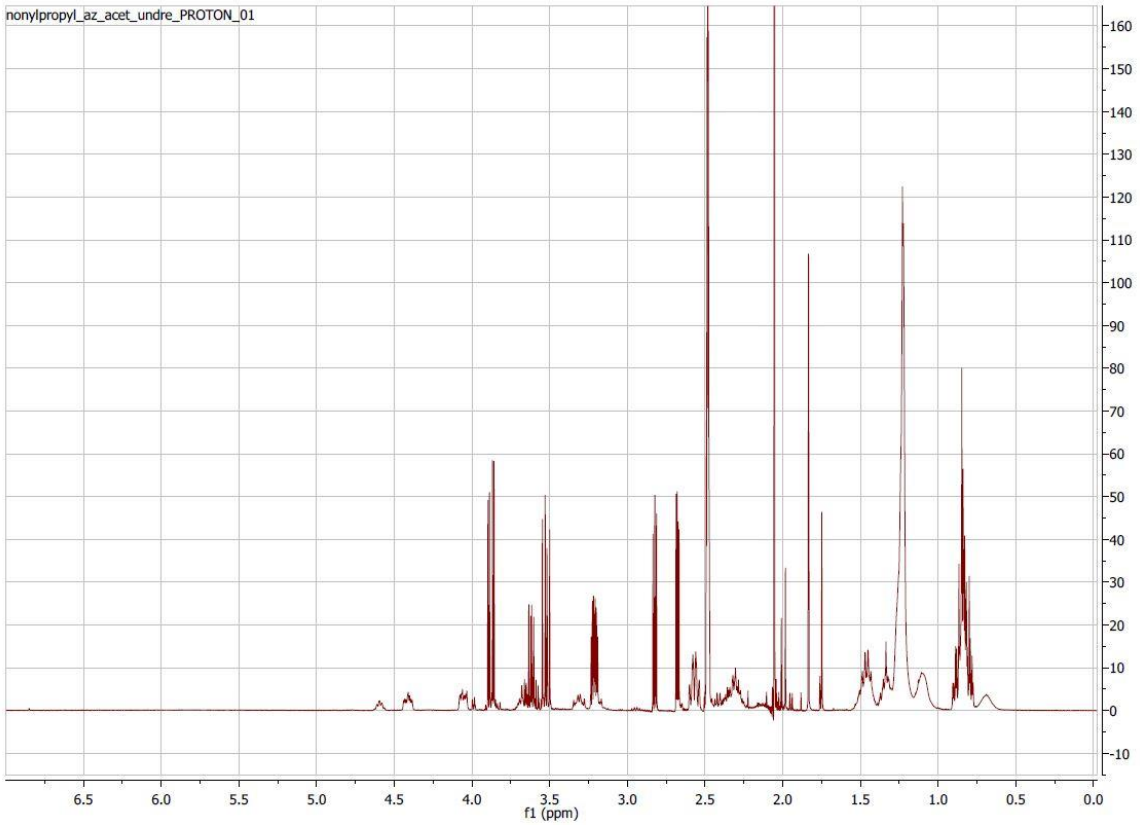

Figure 35: [1]H-NMR spectrum for product 15.

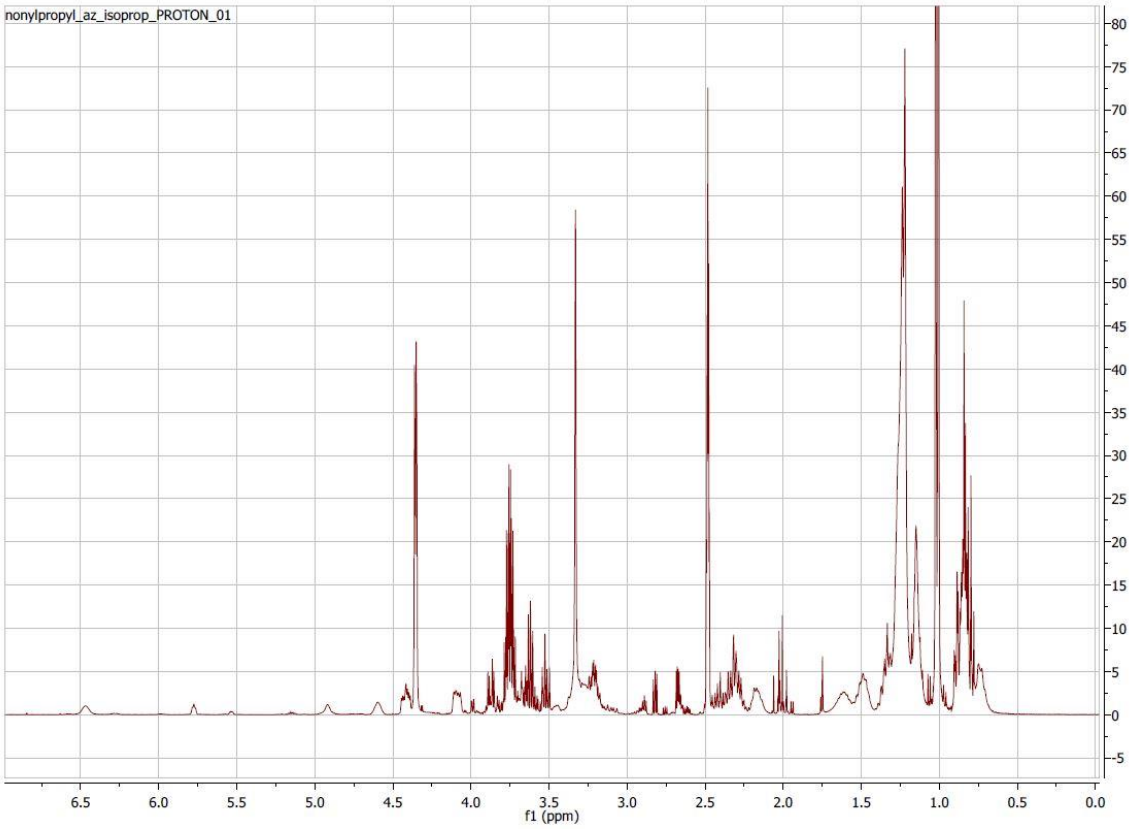

Figure 36: ^{1}H-NMR spectrum for product 16.

B1.6 Undecylmethylazetidinium salt

Chemical structure for Undecylmethylazetidinium salt is shown in figure 37.

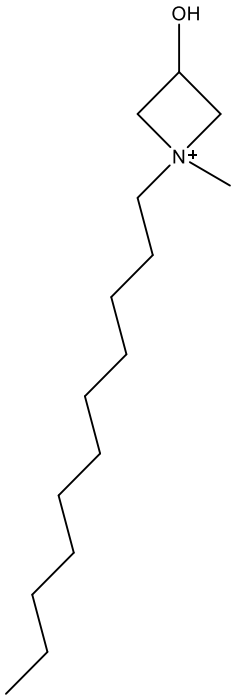

Figure 37: Chemical structure of undecylmethylazetidinium salt.

^{1}H-NMR spectra for product 17 and 18 are shown in figure 38 and 39 respectively. The product in sample 17 were not soluble in DMSO-d_6 due to the long hydrophobic alkali end-group and therefore it was dissolved in $CDCl_3$ instead.

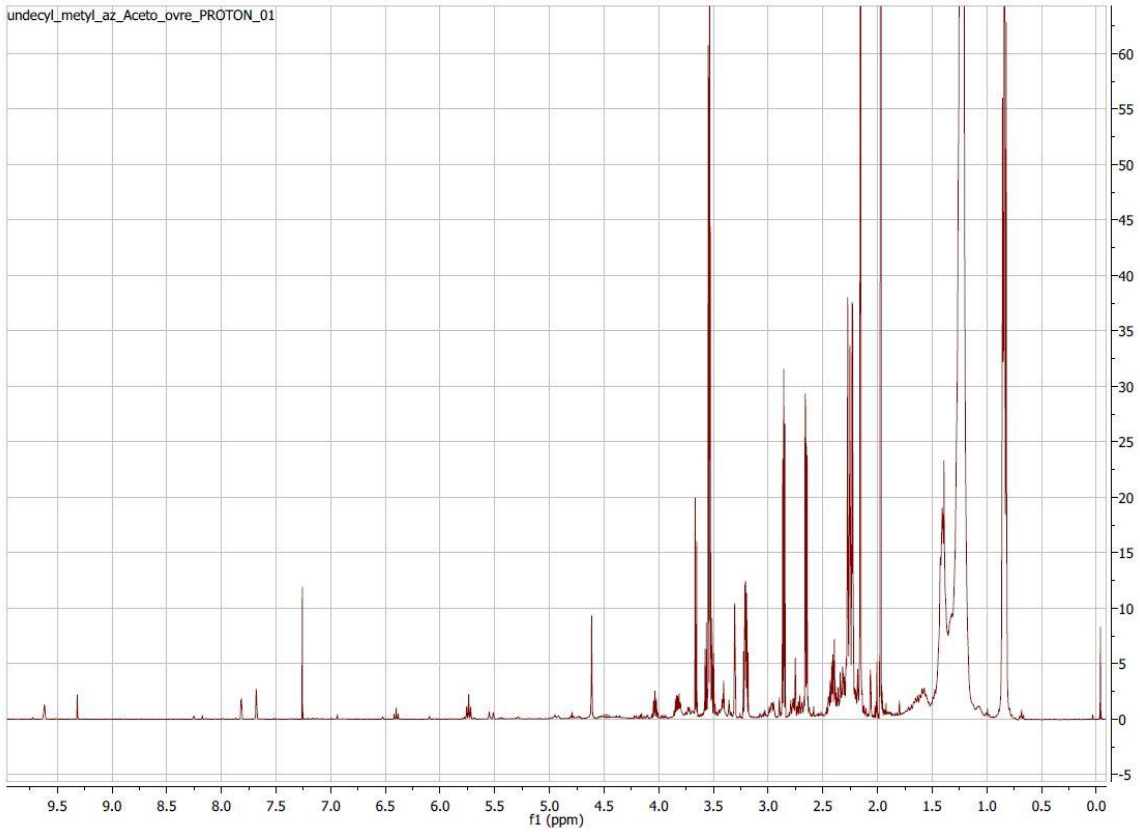

Figure 38: ^{1}H-NMR spectrum for product 17.

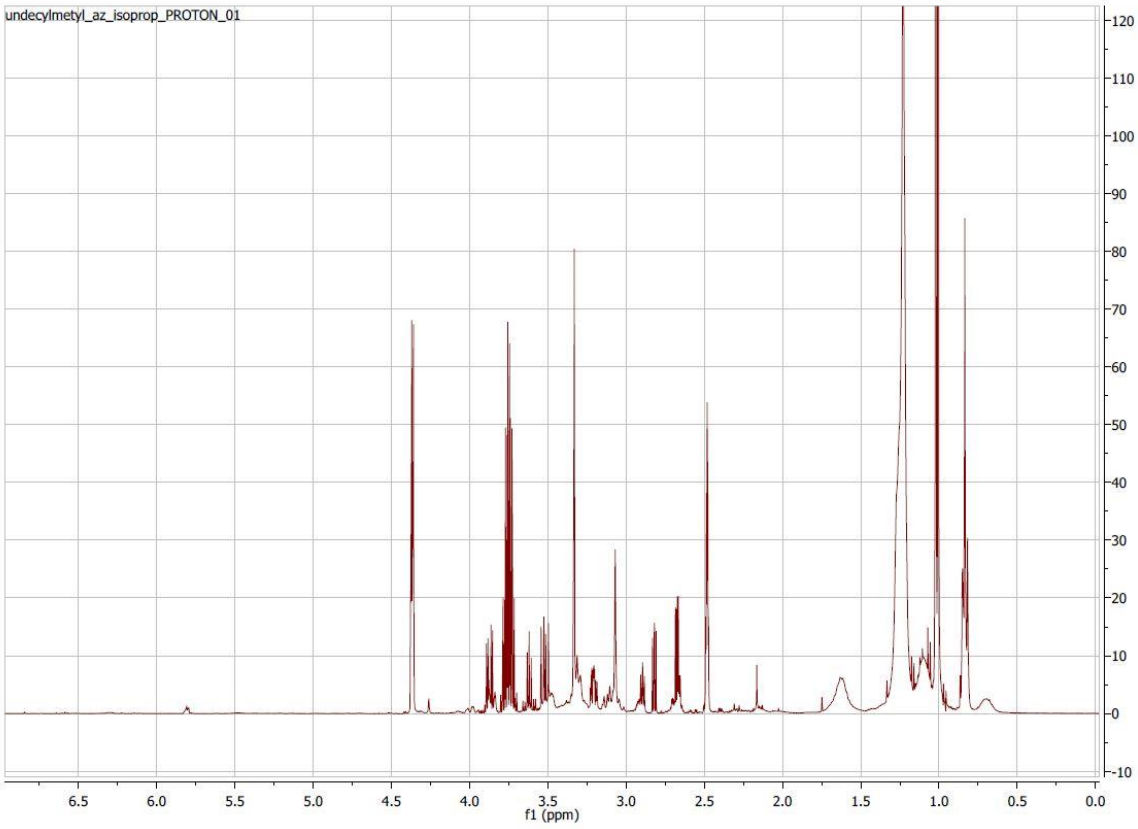

Figure 39: [1]H-NMR spectrum for product 18.

B1.7 Dibenzylazetidinium salt

Chemical structure for dibenzylazetidinium salt can be seen in figure 40.

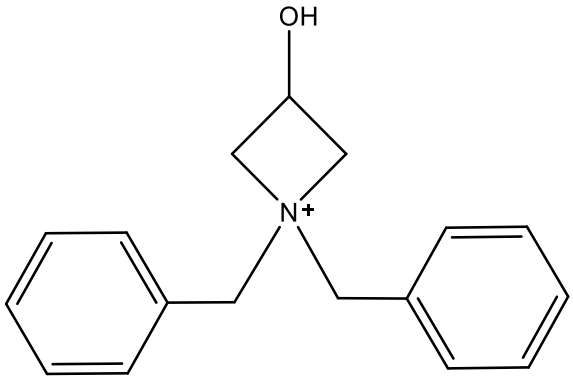

Figure 40: Chemical structure for dibenzylazetidinium salt.

[1]H-NMR spectra for products 19, 20 and 21can be seen in figure 41, 42 and 43 respectively.

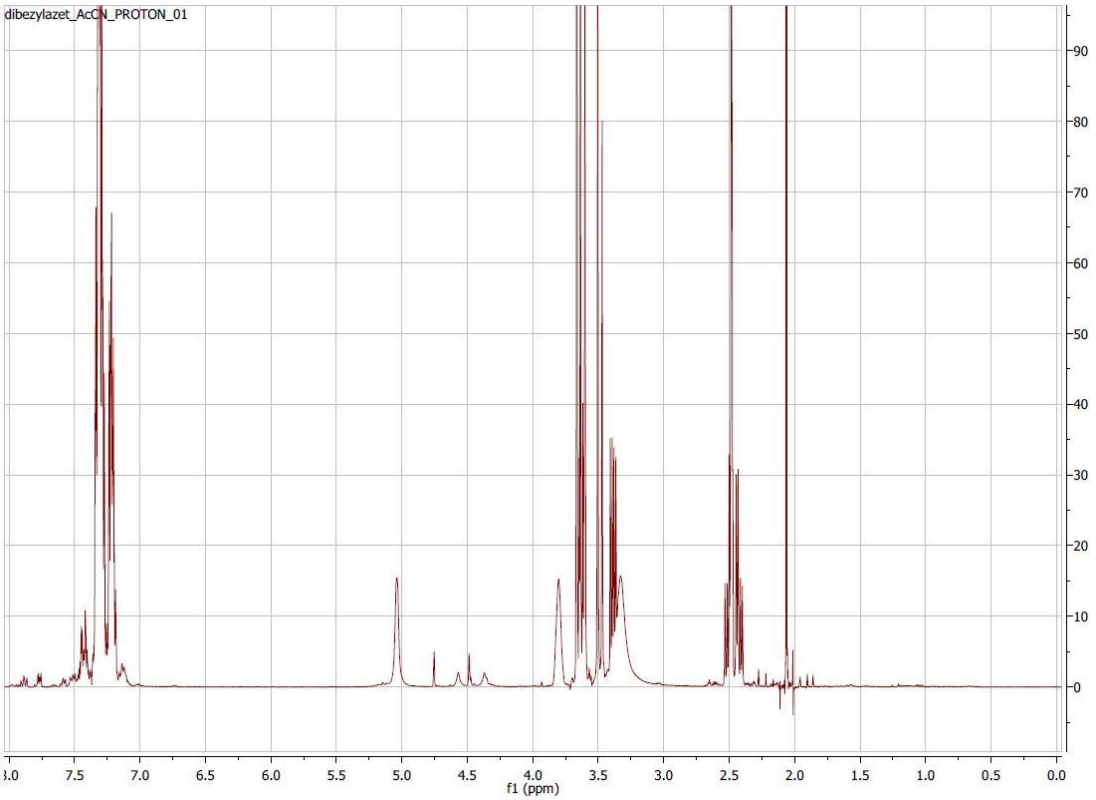

Figure 41: ^{1}H-NMR spectrum for product 19

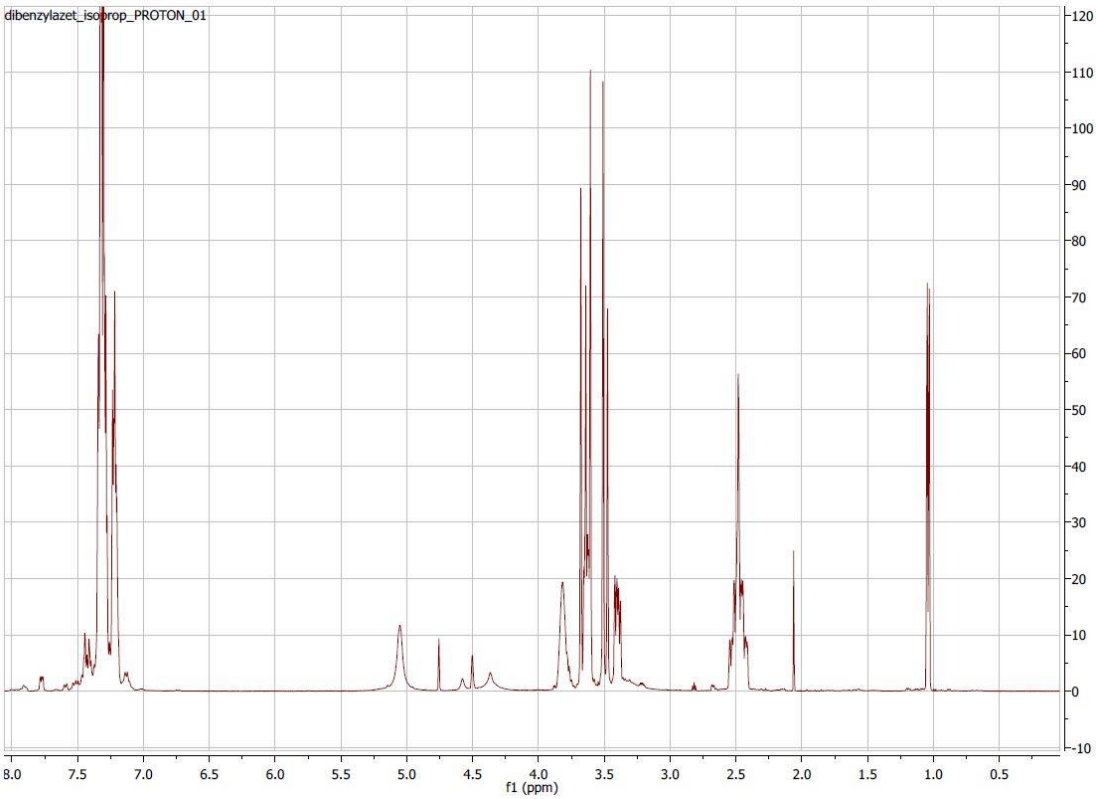

Figure 42: ^{1}H-NMR of product 20.

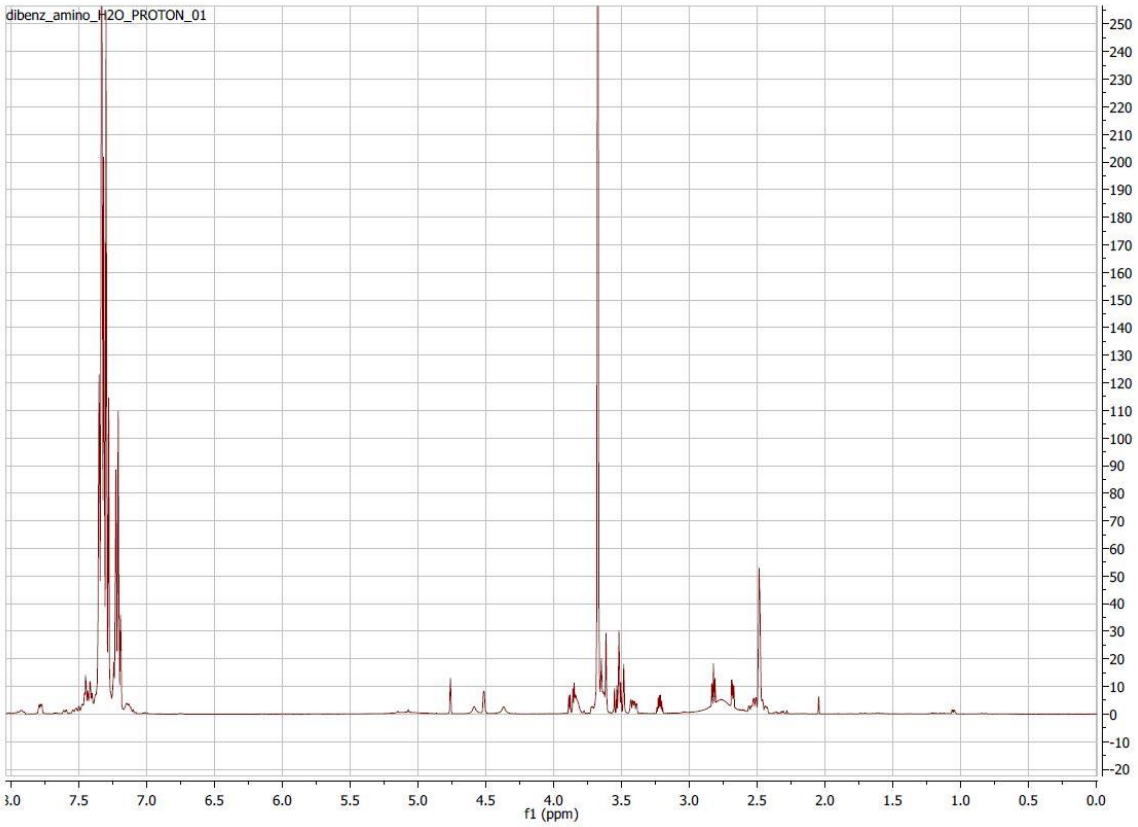

Figure 43: ^{1}H-NMR spectrum for product 21.

B1.8 Nonylpropargylazetidinium salt

Chemical structure of Nonylpropargylazetidinium salt can be seen in figure 44.

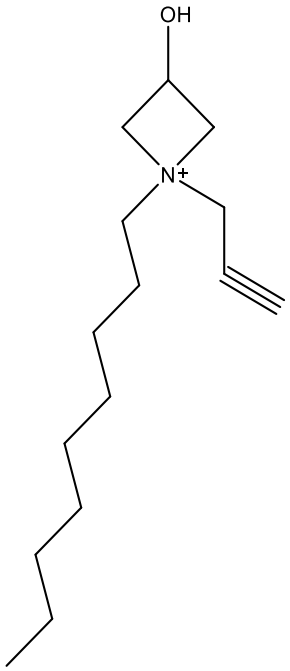

Figure 44: Chemical structure of nonylpropargylazetidinium salt.

^{1}H-NMR spectra for product 22 and 23 are shown in figure 45 and 46 respectively.

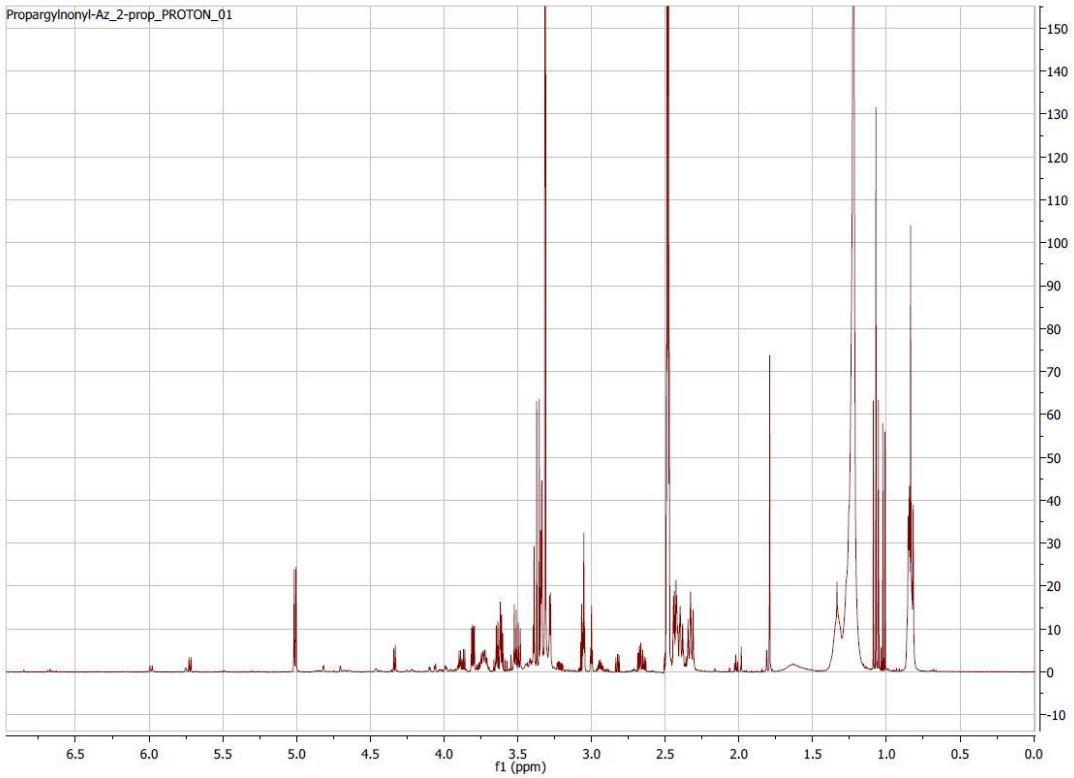

Figure 45: ^{1}H-NMR spectrum for product 22.

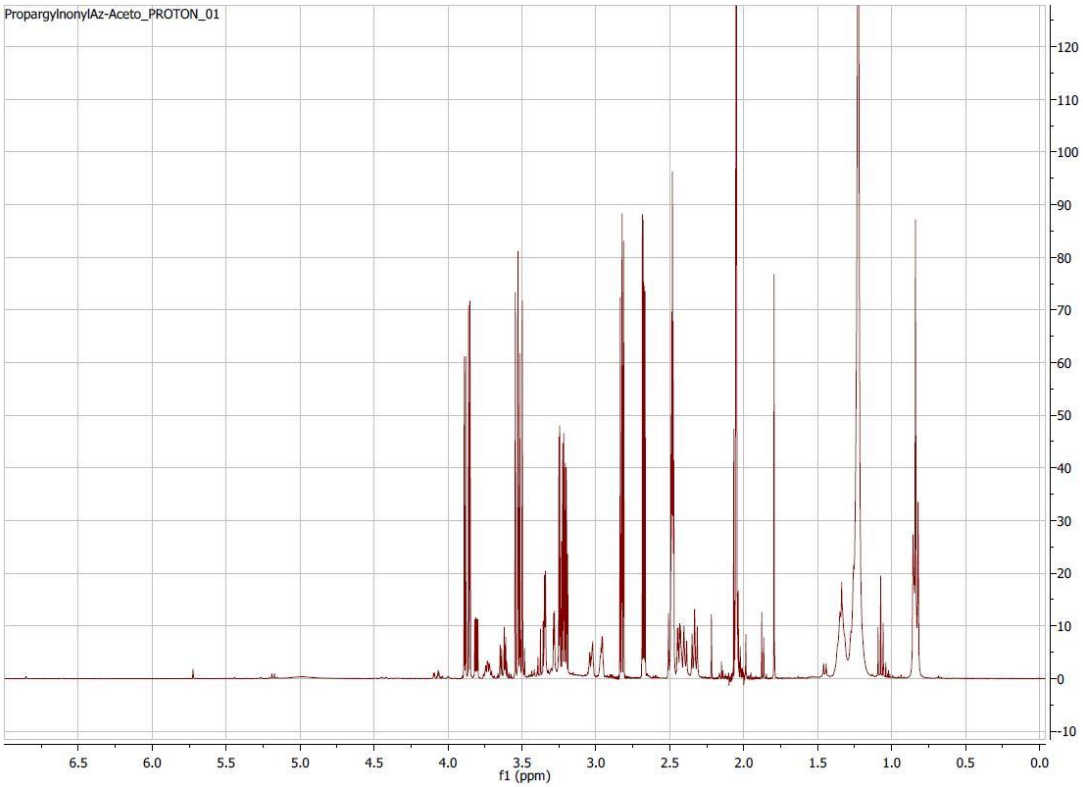

Figure 46: ^{1}H-NMR spectrum for product 23.

B2 – Asymmetrical secondary amines

In this section ^{1}H-NMR results for the synthesized asymmetrical secondary amines will be presented.

B2.1 Benzylpropylamine

The chemical structure of benzylpropylamine can be seen in figure 47 and ^{1}H-NMR spectrum can be seen in figure 48.

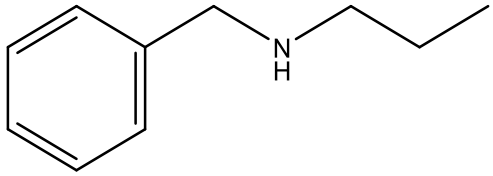

Figure 47: Chemical structure of benzylpropylamine.

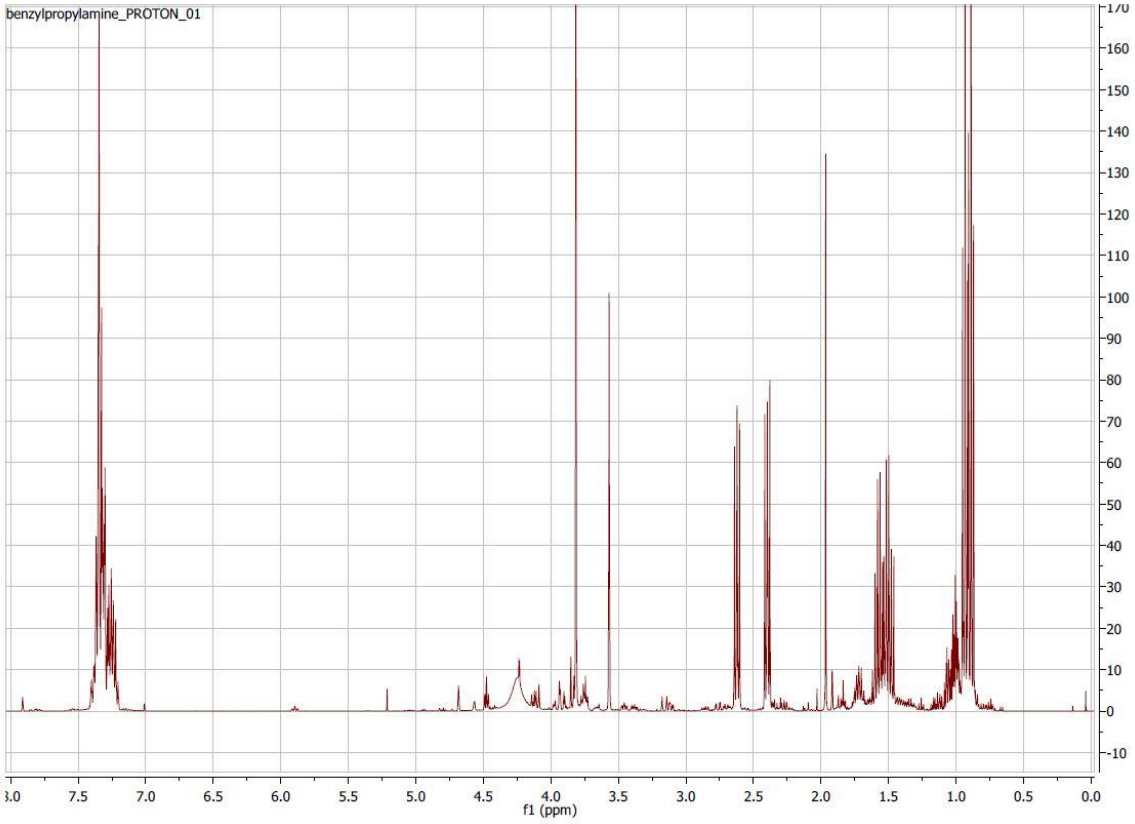

Figure 48: ^{1}H-NMR spectrum of benzylpropylamine.

B2.2 Octylpropylamine

The chemical structure of octylpropylamine can be seen in figure 49 and ^{1}H-NMR spectrum can be seen in figure 50.

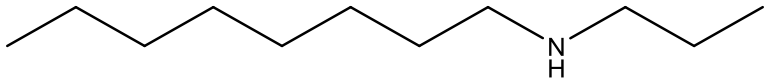

Figure 49: Chemical structure of octylpropylamine.

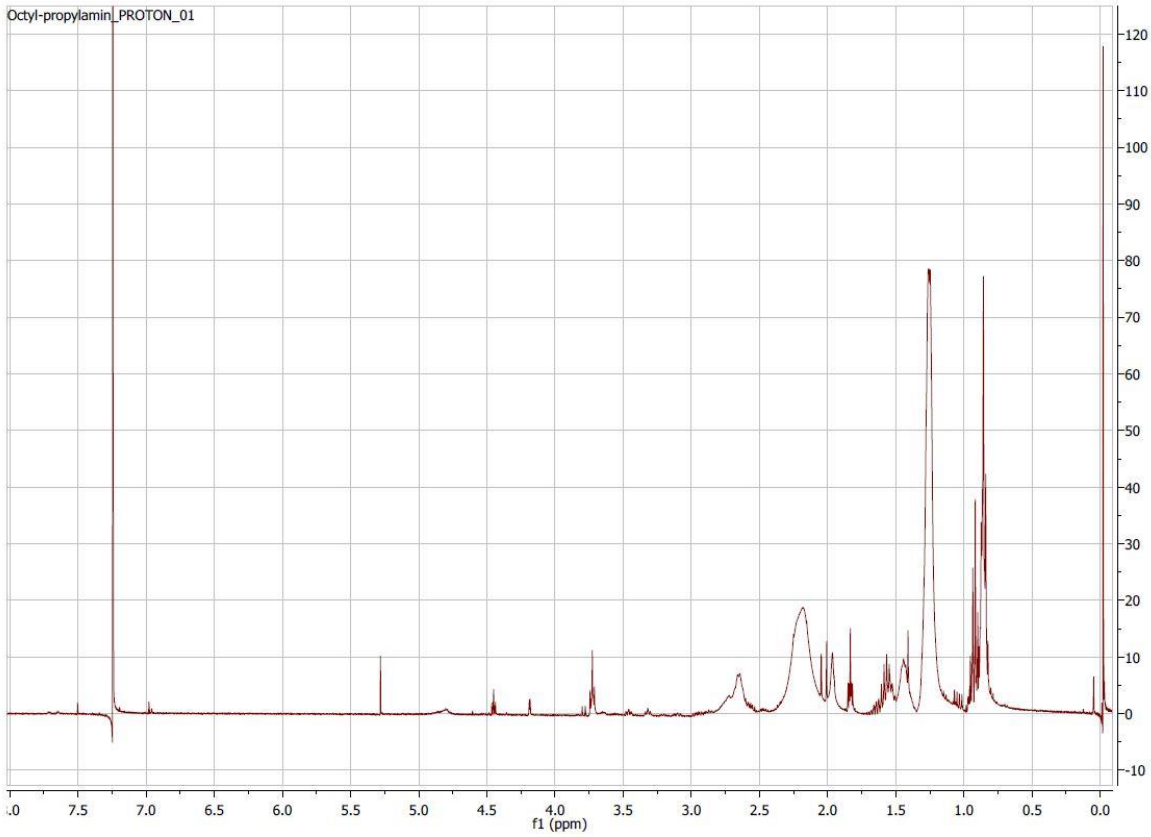

Figure 50: ^{1}H-NMR spectrum of octylpropylamine

B2.3 Nonylpropylamine

The chemical structure of nonylpropylamine can be seen in figure 51 and ^{1}H-NMR spectrum can be seen in figure 52.

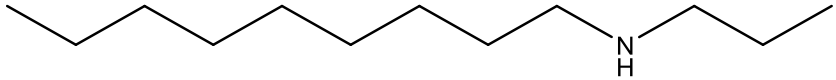

Figure 51: Chemical structure of nonylpropylamine.

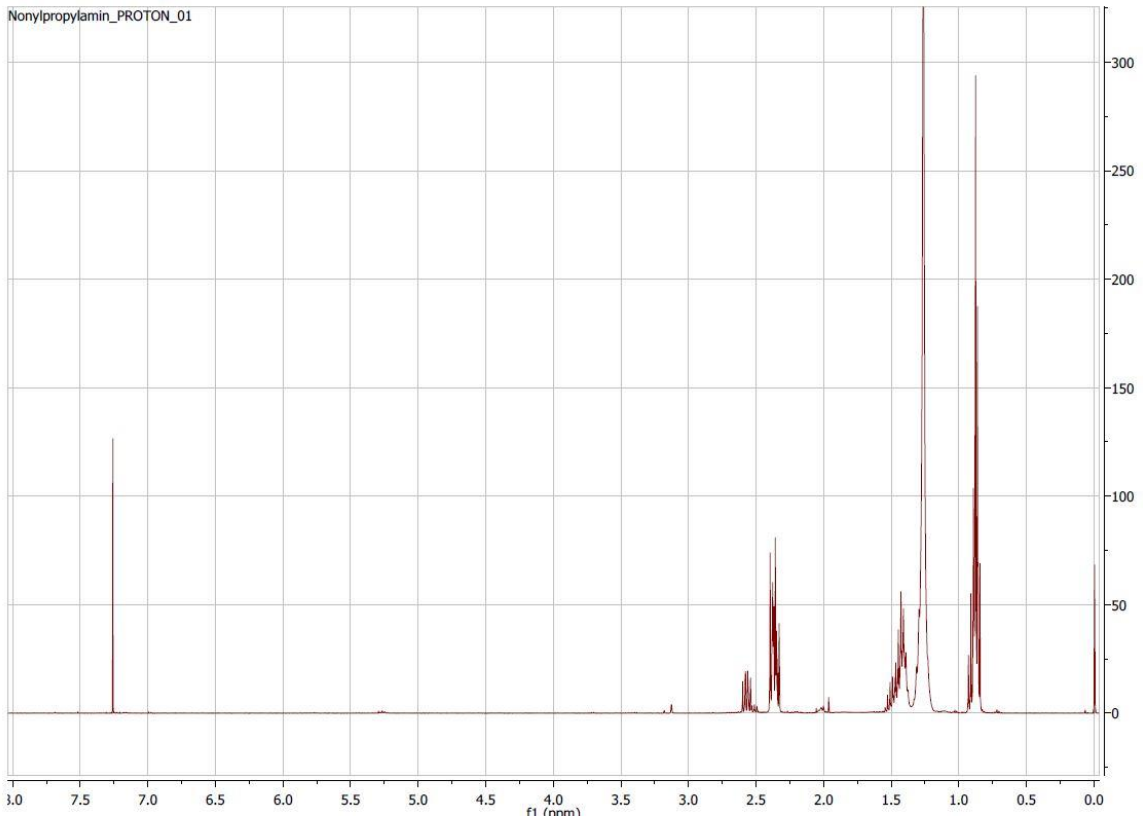

Figure 52: ^{1}H-NMR spectrum of nonylpropylamine

B2.4 Undecylmethylamine

The chemical structure of undecylmethylamine can be seen in figure 53 and ^{1}H-NMR spectrum can be seen in figure 54.

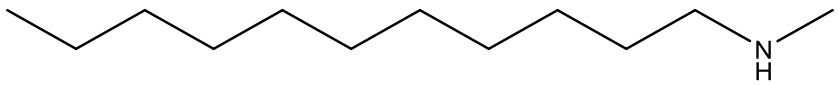

Figure 53: Chemical structure of undecylmethylamine.

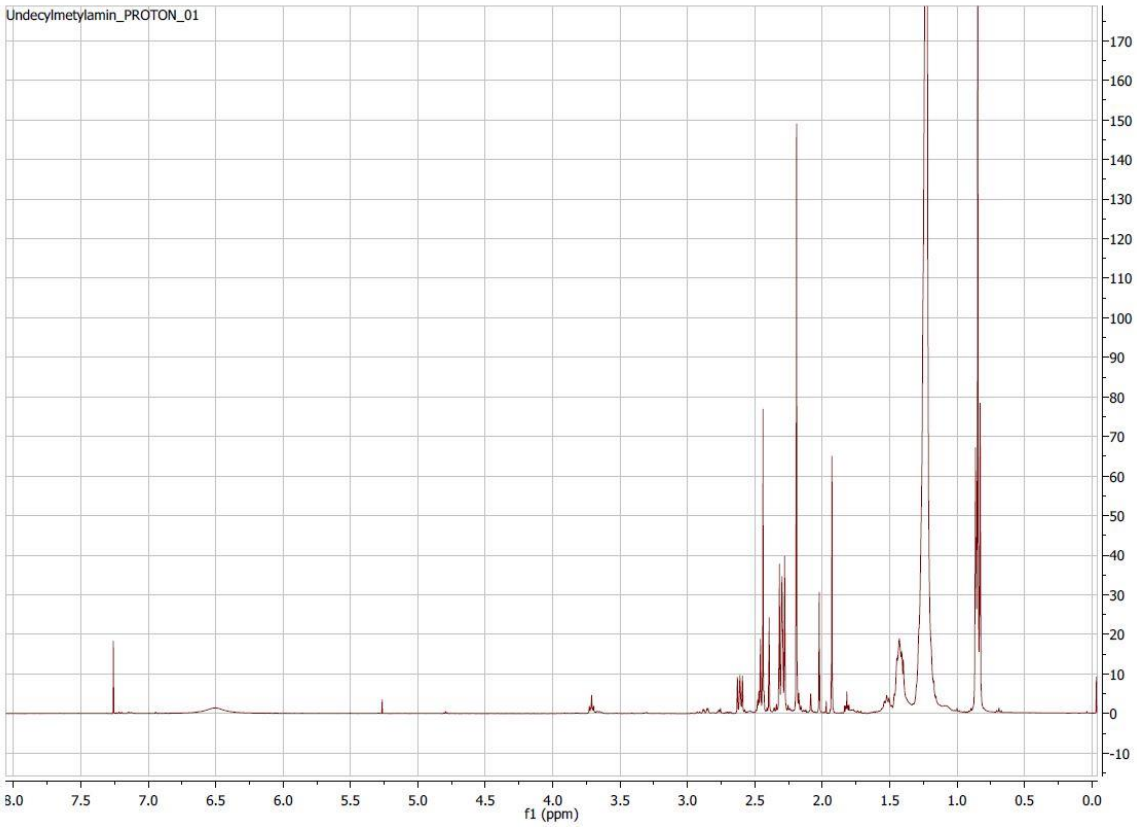

Figure 54: ^{1}H-NMR spectrum of undecylmethylamine.

B2.5 Propargylpropylamine

The chemical structure of propargylpropylamine synthesized with sodium borohydride and *Dowex* cation exchange resin can be seen in figure 55 and ^{1}H-NMR spectrum can be seen in figure 56. ^{1}H-NMR spectrum for propargylpropylamine synthesized with sodium triacetoxyborohydride as reducing agent can be seen in figure 57.

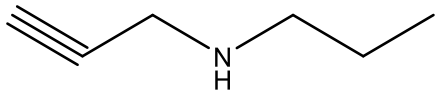

Figure 55: Chemical structure of propargylpropylamine.

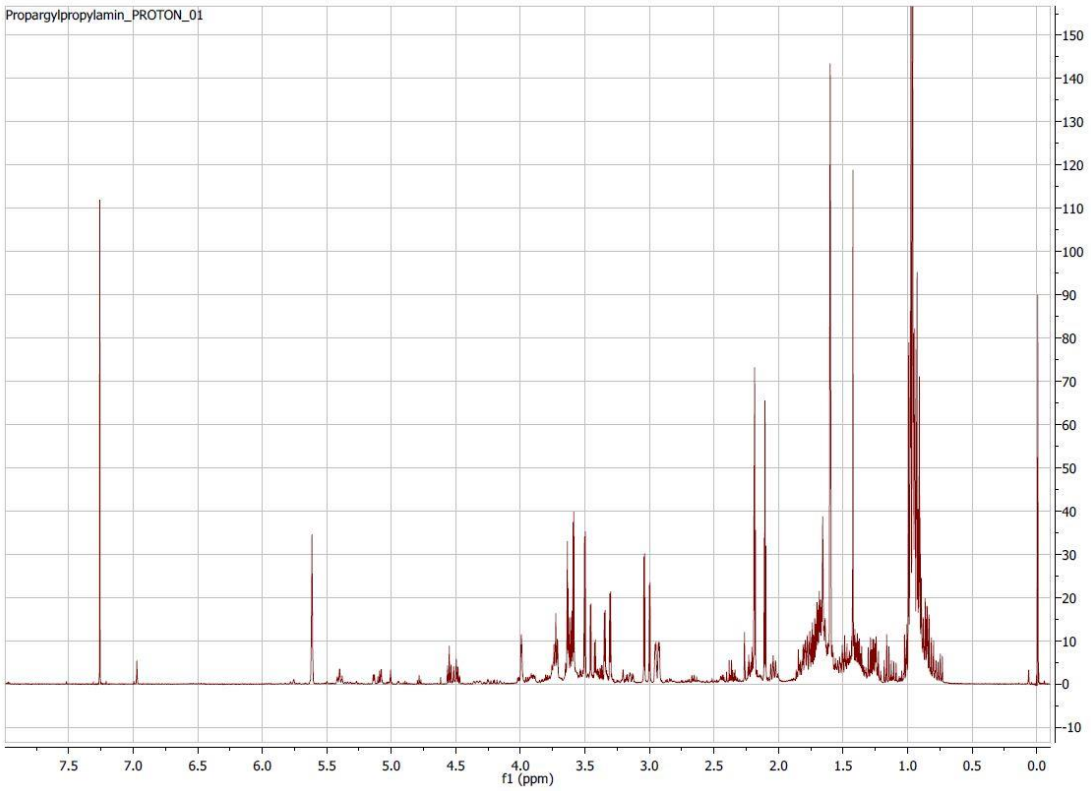

Figure 56: ^{1}H-NMR spectrum of propargylpropylamine synthesized with $NaBH_4$/Dowex as reducing agent.

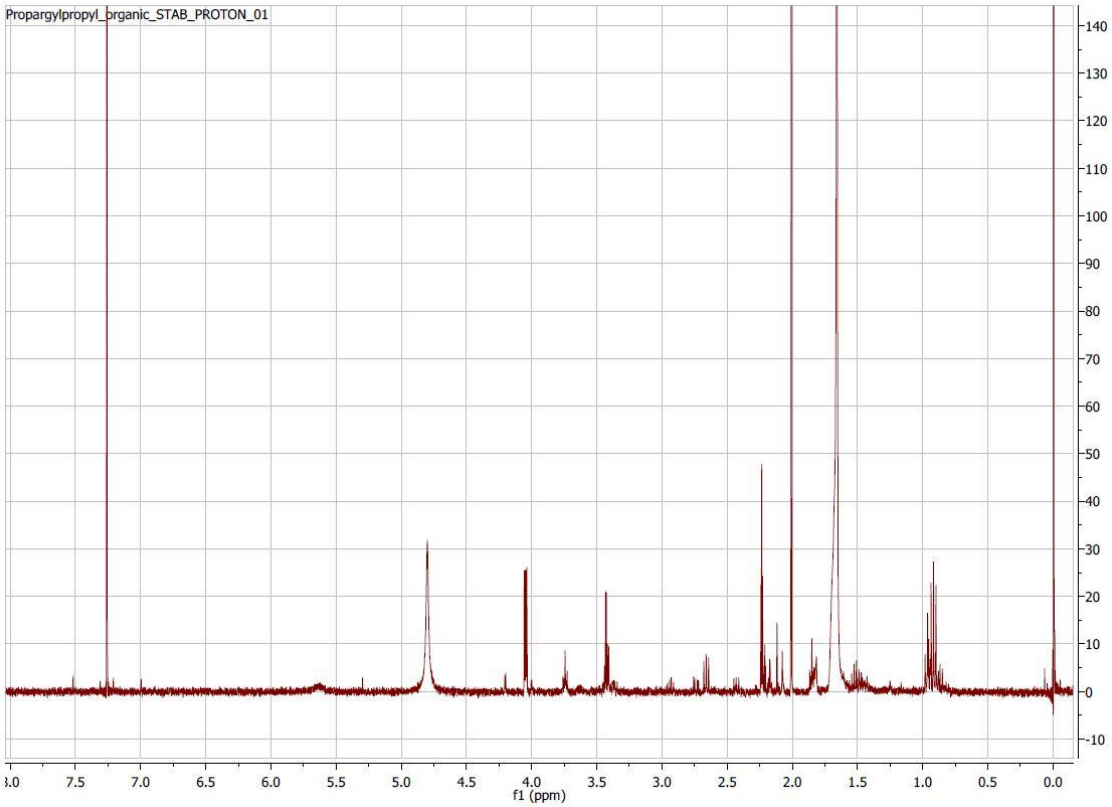

Figure 57: ^{1}H-NMR spectrum of propargylpropylamine synthesized with $NaBH(OAc)_3$ as reducing agent.

B2.6 Propargylnonylamine

The chemical structure of propargylnonylamine can be seen in figure 58 and ^{1}H-NMR spectrum can be seen in figure 59.

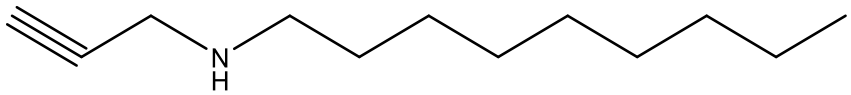

Figure 58: Chemical structure of propargylnonylamine.

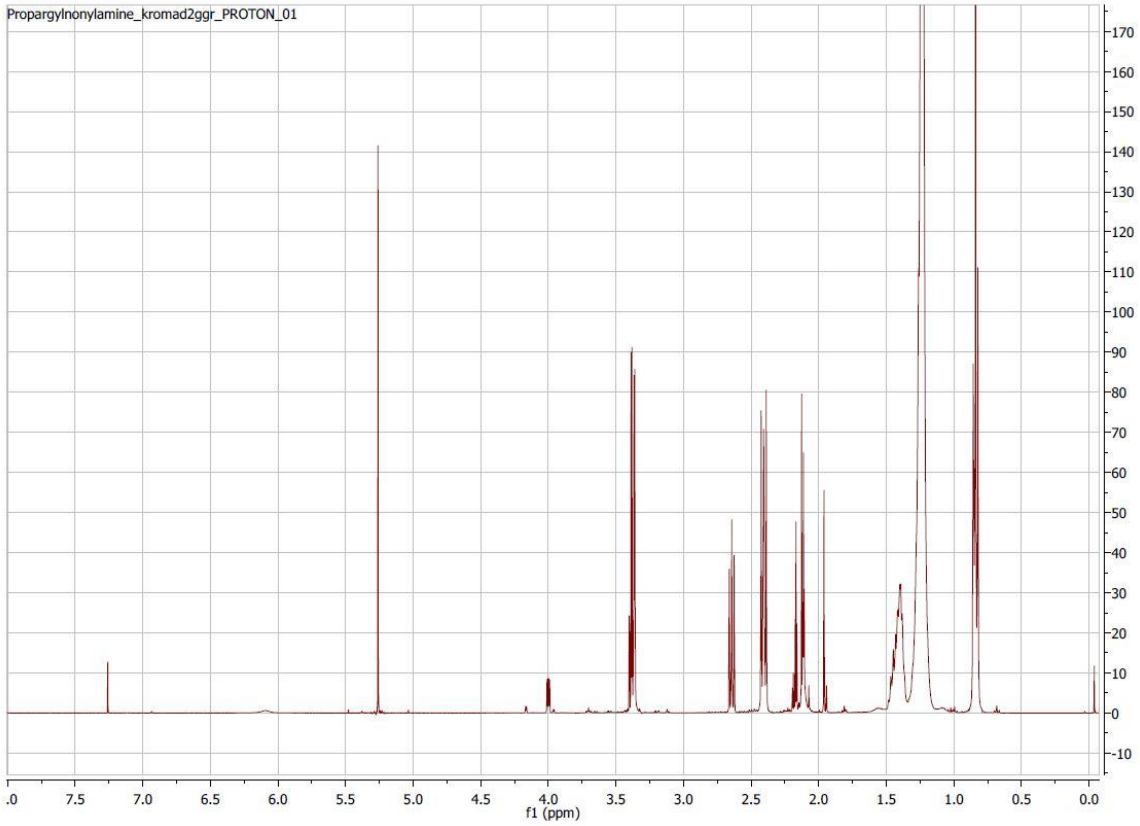

Figure 59: ^{1}H-NMR spectrum of propargylpropylamine.